

NASA/CR-97-

208210

NAGW-4160

Final Report for 1994 - 1997

1N-46-CR

151451

Spatial Relationships  
of Auroral Particle Acceleration Relative to High Latitude Plasma  
Boundaries

NASA Research Grant No. NAGW-4160

Principal Investigator:

Dr. Arthur G. Ghielmetti

Lockheed Martin Missiles and Space  
Advanced Technology Center  
3251 Hanover Street  
Palo Alto, CA 94304

This final report describes the activities under NASA contract to Lockheed Missiles and Space Company. It covers the period from 10.1.94 to 12.31.97. The objective of this investigation is to identify and characterize the spatial relationships of auroral particle acceleration features relative to the characteristic transition features in the surrounding polar ionospheric plasmas. Due to the reduced funding level approved for this contract, the original scope of the proposed work was readjusted with the focus placed on examining spatial relationships with respect to particle structures.

## **1. Summary of Accomplishments**

Appendices A and B provide a copy of the manuscripts of two papers written under this contract to be submitted to JGR for publication. The following brief summary will review the highlights and key results of the work performed under this contract.

### **1.1 Introduction**

The objectives of this investigation are to improve our understanding of the spatial locations of auroral particle acceleration in relation to the magnetospheric plasma regimes and boundaries. The question of the mapping of auroral features from the high latitude polar ionosphere is of fundamental importance to the global morphology of the magnetosphere. In particular the subject of global auroral mapping remains controversial, in part because the instantaneous morphology of the aurora relative to the surrounding plasma boundaries has been insufficiently explored. A mapping from the polar to the equatorial plane is basically difficult, and furthermore there is considerable controversy about the identification of equatorial with high latitude plasma populations.

In this investigation we have used the acceleration signatures in the particle fluxes to infer auroral structures and relate these to specific transition features in the isotropic/precipitating ion and electron fluxes. For this purpose we have analyzed two complementary data sets acquired by the polar orbiting S3-3 and the Viking satellites. These satellites sampled the favorable altitude range between 1 to 2  $R_e$  of the auroral zone where the principal acceleration processes are typically operative. To account for diurnal variations, we have selected two acquisition periods of the S3-3 and the Viking satellite covering the dusk and the dawn local time ranges with good spatial and temporal resolution.

For the dusk LT- study we have used all data acquired by the Lockheed mass spectrometers for a contiguous 40 day sampling period from August to September 1967 covering 63 passes over the northern auroral zone. For the dawn LT study we have used all data acquired by the Hot Plasma Mass Spectrometers from a 40 day period in April and May of 1986 covering 89

passes over the northern auroral one. The two data bases (dawn and dusk ) were then analyzed separately.

For each pass, the latitudinal positions of upward flowing ion events with either field aligned or conical pitch angle distributions were identified and recorded together with their key properties (peak flux and energy). In addition, pitch angle modulation structures in the trapped electron fluxes which are indicative of parallel electric field acceleration above the satellite were identified. Furthermore, for each pass the latitude positions of several typical and recurring transition features in the trapped / precipitating electron and ion fluxes were identified. The data base obtained in this manner provides a means for determining the relative occurrence positions in relation to the "instantaneous" boundaries (transition features) as well as for conducting correlative studies between the various boundaries, acceleration features and other factors such as magnetic activity.

## **1.2 Results**

The principal results of these studies are the following:

### **1.2.1 DUSK- LT Study**

1. Ion and electron acceleration structures extend over a substantial fraction of the hot electron "plasma sheet" (HEP). The latitude extent of particle acceleration increases with geomagnetic activity, reaching on occasion at least ~75 % of the HEP width under magnetically disturbed conditions.
2. The occurrence frequency of particle acceleration increases gradually from the inner edge of the HEP "plasma sheet" to the poleward boundary where it decreases abruptly.
3. The latitudinal distribution of parallel electric field signatures above the satellite is similar to that of the upflowing ion structures, and agrees with the large scale parallel electric field in the plasma sheet reported by Mozer and Torbert [GRL, 1980].
4. The poleward boundary of precipitating energetic protons is on average located poleward of the 1 keV HEP , in agreement with the observations of Lyons et al. [JGR , 1988], who report that discrete aurora generally occur in regions of isotropic energetic ion precipitation.
5. Poleward of the 1 keV electron plasma sheet one finds a latitudinal thin region of energetic proton precipitation (on average ~ 1 ° equivalent to ~ 10% of the HEP width) coincident with and a wider region of cold highly structured electron fluxes. A mapping of the "plasma sheet boundary layer" observed at > 20 Re to this high altitude polar region seems appropriate..
6. At dusk and altitudes of ~ 1 Re auroral ion and electron acceleration structures are located predominantly within the HEP "plasma sheet" region. Acceleration structures may occur anywhere from the low latitude edge to the high latitude boundary of the HEP "plasma sheet" but with a clear preference for the high latitude 50% portion of the HEP. Thus the UFI occurrence distribution is centered in the outer \_ portion of the HEP

plasma sheet, a region that may be associated with the boundary plasma sheet (BPS).

7. On a orbit by orbit basis the latitude width of auroral particle acceleration exhibits large variations. However, the latitude extent increases both absolutely and relatively with respect to the HEP width with geomagnetic activity.
8. Based on the generally recognized association between discrete auroral arcs, parallel electric fields and ion and electron acceleration signatures in the particle distributions we conclude that a.) the high latitude HEP plasma sheet maps to the auroral oval, and b.) that the large majority of discrete auroral arc and inverted V acceleration structures occur within this HEP plasma sheet.
9. The latitude occurrences of particle acceleration signatures is well ordered by the HEP region and moves in concert with its "boundaries".
10. The majority of particle acceleration structures occur at lower latitudes than the "electron trapping boundary" (ETB), that is on field lines that show the typical signatures of a closed magnetic field line configuration.

### **1.2.2 DAWN - LT Study**

1. On the dawn side, the zones of upflowing ions extend typically over about  $5^\circ$  in invariant latitude on average. This is considerably wider than the typical width of an arc or of an inverted V structure. The frequency of occurrence for such wide structure is surprisingly high considering that discrete auroral arc are primarily dusk - side phenomenon.
2. The latitude position of the ion upflow regions is ordered by and moves in concert with the poleward boundary of the contiguous hot ion flux region (PIB).
3. The UFI occurrence frequency distribution is centered about this PIB transition boundary. The width of the UFI distribution with respect to the instantaneous PIB location is considerably narrower than the width of the distribution seen in absolute latitude. Thus the UFI acceleration regions are closely coupled to the PIB boundary.
4. The locations of the PIB and the hot contiguous electron boundary (PEB) are well correlated, with the PIB being on the average about  $1.5^\circ$  further poleward.
5. The average width of ion upflow increases considerably with magnetic activity.

### **1.3 Conclusions**

The work conducted under this contract provides important new information on the spatial relationships of auroral particle acceleration in relation to high

latitude plasma boundaries. It provides a frame for a mapping of the key high latitude acceleration regions to the equatorial magnetosphere, through their association with distinct and well recognizable features in the plasma populations and their transition features. The implications of this work are that at dusk and dawn local times the mapping is primarily through the region of hot isotropic/precipitating electron and ion fluxes. In the dusk LT region this mapping is often on closed field lines. At dawn, auroral acceleration is tied to the poleward transition boundary of the hot isotropic ion fluxes.

In either cases, the "instantaneous" latitude width of the acceleration structures spans a substantial portion of the hot electron/ion population region, indicating that the primary mapping of acceleration structures is not through the plasma sheet boundary layer the latitudinal width of which, when projected to the polar ionosphere, is expected to be much thinner. However, the low altitude ionospheric projection of the plasma sheet boundary layer has been insufficiently researched thus far and needs to be investigated in further detail with more sensitive instruments before final conclusions may be drawn. Furthermore, significant differences have become apparent in the relations of acceleration structures to the plasma transition boundaries of the polar ionosphere between the dawn and dusk LT sectors which are presently not understood.

## **2. Future Work**

The frequent presence of acceleration processes with substantial latitude width as reported here tends to modify the hot trapped particle distributions as well. Thus relationships derived from within the altitude range where the acceleration process are operative must be interpreted with caution. What is now necessary is to conduct similar studies of the polar ionosphere from higher orbiting polar platforms. This remains an ideal topic for detailed research with the POLAR spacecraft which carries highly sensitive ion mass spectrometers capable of high time resolution measurements. A comparison of the relationships derived at the 8000 km altitudes with relationships derived at higher polar altitudes and with more sensitive instrumentation would permit to refine the mapping process initiated here. This work is beyond the scope of the current contract.

---

Arthur G. Ghielmetti



Spatial Relationships  
of Auroral Particle Acceleration Relative to High Latitude Plasma  
Boundaries

Part I : "Pre-Midnight Local Time Sector"

A.G. Ghielmetti and J.M. Quinn\*

Spaces Sciences Laboratory  
Advanced Technology Center  
Lockheed Martin Missiles and Space

\* University of New Hampshire

## Contents

1. Introduction .....	3
2. Experiment .....	4
2.1 Data Selection and Analysis.....	5
2.2 Ambient charged particle boundaries.....	5
2.3 Particle acceleration structures .....	7
2.4 Analysis Method .....	8
3. Results .....	8
4. Discussion.....	10
5. Summary and Conclusions.....	11

## ABSTRACT

Charged particle data from the hot plasma composition experiment aboard the polar orbiting satellite S3-3 have been analyzed to investigate the structure and location of auroral acceleration regions in relation to the spatial boundary in the trapped and precipitating ion and electron fluxes in the high altitude polar

ionosphere. The principal conclusions drawn from this study are that the ion and electron acceleration regions occur predominantly within the plasma sheet and typically extend over a substantial portion of the plasma sheet width as viewed on a single pass basis. During magnetically disturbed periods the latitudinal extent of particle acceleration expands and to cover a major latitude portion of the polar region carrying typical plasma sheet ion and electron fluxes. Not infrequently these signatures are observed down to near the inner edge of the high latitude extension of the plasma sheet. This suggests that the ionosphere auroral ion and electron acceleration regions map to the entire plasma sheet, with a higher occurrence probability toward the outer (high latitude) portion. As a consequence, ionospheric ions are often directly injected into a latitudinal wide section of the plasma sheet. The latitude width of the acceleration & ion injection regions cover a significant portion of the total plasma sheet latitude extension. Acceleration events are not limited to a relatively thin boundary at the polar side of the plasma sheet, as suggested by the boundary layer model. The observations are consistent with at least some of the field aligned ion fluxes seen in the equatorial plane near geosynchronous orbit having originated from events occurring near the equatorward high altitude plasma sheet edge in with little or no radial transport.

## 1. Introduction

The recent spectacular results from the NASA's POLAR ISTP mission have renewed the interest in the global morphology of auroral processes. A key motivation behind these studies is to understand how auroral features map from the polar ionosphere to the equatorial and tail magnetosphere. Presently several competing interpretations of auroral mapping are being discussed. The leading interpretations may be broadly summarized in terms of three principal ideas: 1- The near earth neutral line substorm model (NENL), which involves the formation of a new neutral line close to the earth. Here the equatorial substorm breakup arc would map to the neutral line ( McPherson et al 1973, Hones 1984, Nishida et al 1988). 2. The boundary layer dynamics substorm model (BLD) in the mapping is along the plasma sheet boundary layer (Rostoker and Eastman 1987, Frank and Craven 1988). 3. Finally a mapping of the nighttime auroral oval to the central plasma sheet with the equatorial edge of discrete arcs mapping to the equatorward edge of the equatorial plasma sheet, that is to a position near the injection boundary ( McIlwain 1974, Mauk and Meng 1983, Galperin and Feldstein 1991). These conflicting interpretations illustrate how despite significant progress the mapping between the polar ionospheric regions and the equatorial regions remains elusive.

The objectives of the current investigation are to improve the understanding of the relationships between the spatial occurrences of typical acceleration features seen in the particle fluxes and the characteristic transition features in the surrounding plasmas of the polar ionosphere. The high latitude ionosphere can be surveyed in a relatively short time span from a polar orbiting satellite providing a high time resolution ( on a single pass basis) cross section of the prevailing spatial structures. Since the polar ionosphere is magnetically connected to the equatorial and tail regions of the magnetosphere a mapping of these structures on an "instantaneous basis" is in principle conceivable.

Past morphological studies of upward flowing ions have shown that the high latitude ion acceleration region is statistically coincident with the auroral oval. These studies, however, do not directly describe the spatial relationship between acceleration structures and the magnetospheric regions in which they occur. In order to resolve this question, we have examined the ion and electron data acquired near dusk and near dawn by the polar orbiting S3-3 satellite. At these local times, the electron fluxes provide

a convenient means of identifying the poleward and equatorward edges of the high latitude extension of the plasma sheet.

A number of large scale statistical investigations have determined the absolute latitudinal position of auroral zone phenomena (e.g. particle precipitation, particle acceleration, electrostatic shocks, currents). However, only few studies exist that explore the instantaneous locations of particle acceleration structures relative to magnetospheric boundaries. Such global investigations of the "instantaneous" auroral morphology are ideally conducted from polar orbiting satellites that provide rapid sampling of the high latitude high altitude ionosphere.

This study is structured into two complementary parts: Part I describes the spatial relationships observed in the dusk local time sectors, while the dawn local time region relationships are described in Part II.

## 2. Experiment

In this study we examine the latitudinal locations of auroral acceleration signatures in the particle distributions relative to the plasma boundaries in the isotropic or precipitating fluxes observed during the same orbital segment ("instantaneous"). Specifically, we use the observations of upward flowing ions (UFI) and electron pitch angle modulation signatures (Cladis and Sharp, JGR 1979) as diagnostics of large scale auroral particle acceleration structures. While the former (UFI) imply acceleration structures located below the satellite, the latter are indicative of parallel electric fields located at higher altitudes.

To gain a comprehensive view by means of in situ particle measurements requires a large number of orbital passes from a global picture is reconstructed. Since we use particle acceleration signatures to identify aurora structures, it is essential that the observations be made in the altitude range where these processes are operative, that is typically above 1 Re. Furthermore, to investigate the "instantaneous" spatial interrelationships between the different particle structures requires fast traversal of the auroral zone. The polar orbiting S3-3 satellite with apogee at 8000 km, and the Viking satellite with apogee at about 12000 km both meet these orbital requirements. A typical auroral zone traversal required about 5 minutes for the S3-3 satellite and about twice as long for the Viking satellite, thus providing sampling on time scales short compared to typical substorm decay times.

For the purpose of this investigation we have selected two complementary data sets, one acquired by the S3-3 satellite in the dusk LT sector, and the other obtained by the Viking satellite at dawn LT. These two experiments provided extensive data bases of particle observations above the northern and southern hemisphere high latitude ionosphere during a combined period of about 3 years. The specific acquisition periods selected are of nearly equal length (~ 40 days) and contain a large number (63 and 89) orbital segments that meet the altitude-local time constraints. Microfiche spectrograms were visually scanned for signatures of upflowing ions, electron pitch angle distributions, and for the presence of isotropic (precipitating) fluxes above a threshold level. Each contiguous region of ion upflow (or electron pitch angle modulation) was characterized by its extent in invariant latitude, and its relation to several plasma boundaries defined further below.

Although there is an association between visible discrete auroral arcs and particle acceleration structures (inverted V's) the latter are known to have significantly wider

latitudinal extent. Such inverted V's may not of necessity give rise to visible discrete auroral arcs. This suggests that studies Mapping based exclusively on optical observations of discrete arcs may therefore be biased toward the more intense acceleration regions, and/or toward special conditions prevail that are give rise to discrete arc features. In fact, the frequent reference to discrete arcs being located at or near the polar cap boundary suggests

Within the 1 Re altitude range in the auroral ionosphere [ionospheric ions are commonly accelerated to energies ranging from a few eV to > 16 keV. Upward flowing ions with either field aligned (beams) [Shelley et al., 1976; Mizera and Fennell, 1977], or conical pitch angle distributions (conics) [Sharp et al., 1977, Whalen et al., 1978; Yau et al., 1983, Klumpar 1979 ], are generated primarily at high altitudes above the auroral region.

## **2.1 Data Selection and Analysis**

The data used in this study were acquired by the Lockheed energetic particle experiment aboard the polar orbiting S3-3 satellite. Spin axis and experiment view directions were oriented such that complete pitch angle scan to within about 5° of the magnetic field lines were obtained every ~ 20 seconds. Three ion mass spectrometers simultaneously scanned the mass range from 1 through 32 AMU /charge in about one second at exponentially space energy levels. Approximately once every spin period, the energy levels were stepped to one of four values thus covering the energy range from 0.5 to 16 keV once every 64 sec. In addition, four broad band electron spectrometers provided contiguous coverage of the energy range from 70 eV to 24 keV with a temporal resolution of 0.5 seconds. Both ion and electron instruments have rather narrow (+-3 ° FW) angular acceptances which make them suitable for observing anisotropy pitch angle distributions resulting from auroral acceleration processes. More detailed descriptions of the instrumentation are available from Sharp et al. [1979].

The S3-3 satellite was in an elliptical polar orbit with apogee at ~8000 km altitude. With a period of its polar orbit was about 3 h, the satellite traversed the key particle regions of interest (radiation belts, ring current, auroral zone, and the high latitude extension of the plasma sheet) in the relatively short time span of about 20 minutes (Fig 1).

To limit the sampling to the dusk high altitude auroral acceleration region we have selected a contiguous period of S3-3 data acquisition from August 18 to September 29, 1976. During this 43 day period, a total of 60 orbital passes that met the acceptance criterion of providing sampling of the local time region from 16.00 to 20.00 MLT at altitudes above 6000 Km, and over the latitude range from 60 to 85 ° ILA were obtained. This period is characterized by generally low magnetic activity although two smaller magnetic storm occurred during this period. The period is near the minimum of the solar cycle.

Microfiche data in the form of energy time survey plots of the type shown in Ghielmetti et al [1979] were examined visually for signatures of upward flowing ions (UFI), electron acceleration structures and the presence of isotropic fluxes above a threshold level. These microfiche plots provide integral flux versus time spectrograms for 4 electron (70 eV to 24 keV) and 12 ion energy (0.5 to 16 keV) channels for 4 masses, as well as pitch angle information. For each type of event described in more detail below its MLT, ILA range, UT, Kp, and the energy at which signature was observed were registered.

## **2.2 Ambient charged particle boundaries**

To characterized the ambient energetic isotropic plasma fluxes we introduce the following "boundary" definitions for the ambient plasmas:

1. The **low latitude hot electron (equatorward) boundary (EEB hot)** : The most equatorward occurrence of the  $> \sim 1$  keV trapped or isotropic precipitating electron fluxes.  
["inner edge of hot electron plasma sheet"]
2. The **high latitude (poleward) hot electron boundary (PEB hot)**: The most poleward occurrence of the  $> \sim 1$  keV electron fluxes.  
(poleward boundary edge of "hot electron plasma sheet")
3. The **high latitude (poleward) cold electron boundary (PEB cold)**: The most poleward occurrence of  $\leq 0.24$  keV electron fluxes.  
(poleward boundary edge of "cold electrons")
4. The **electron trapping boundary (ETB)**: The most poleward occurrence of anti-loss cone pitch angle distributions in the electron fluxes.  
(electron trapping boundary)
5. The **poleward ion boundary (PIB hot)**: The most poleward occurrence of energetic ( $> \sim 6$  keV) proton fluxes.  
(poleward edge of plasma sheet).

Following Vasilyunas [1968], Frank [1971], and Shield and Frank [1970] the equatorward boundary of the hot electron fluxes is as in the equatorial plane assumed to be associated with the inner edge of the plasma sheet. As discussed by these authors, the lower energy electrons ( $< 5$  keV) regularly exhibit a flux minimum in the latitude range from  $60$  to  $70^\circ$  ILA at dusk LT. This

The low latitude boundary of the hot electron fluxes (**LEB hot**) is identified from a decrease in the energy flux of the  $> 1$  keV electrons. These electrons as observed in the S3-3 data often exhibit typical energy dispersion features which are consistent with those reported for the equatorial plane [Horwitz, 1986, ]. The lower energy electrons are typically seen to extend further inward (to lower latitudes). Occasionally the electrons fluxes may exhibit a sharp cutoff as in the example in Ghielmetti et al [1979].

The electron trapping boundary (**ETB**) represents the most poleward latitude of anti-loss cone pitch angle distributions in the electron fluxes. Equatorward of the LEB, electrons typically exhibit anti loss cone pitch angle distributions at all energies (70 eV to 24 keV); while poleward of the EEB the low energy electrons have isotropic precipitating pitch angle distributions. Since parallel electric field located above the satellite can trap and mirror lower energy electrons, downward loss cone pitch angle distributions at low energies are not necessarily indicative of closed field lines. For these reasons we rely exclusively on the two highest energy electron (1.6 to 23 keV) channels for defining the "electron trapping boundary". In cases where these channels exhibit the typical signatures of inverted V events their pitch angle information is not used for defining an "ETB" boundary. Not infrequently, filled in downward loss cones are observed equatorward of the most poleward occurrence of anti loss cones. To distinguish loss cone structures from spatial - temporal variations in the particle fluxes we require that the anti loss cone signatures persist for a least two consecutive spins.

The poleward electron boundary (**PEB**) represents the most poleward occurrence of energetic electron fluxes. At high latitudes the electron fluxes may exhibit large intensity fluctuations with "temporary" drops below the instrument sensitivity threshold. These fluctuations are more pronounced in the low energy electrons ( $< 1$  keV). However, The

more energetic particle fluxes typically decrease gradually or abruptly to below instrument sensitivity level without a recurrence at higher latitudes. In order to provide a clear definition of a poleward boundary we define of the PEB used in part I of this paper and use the for this purpose the 2 highest energy channels ( $> 1.5$  keV). Since the low energy electrons ( $< 25$  keV) extend typically further poleward, and in order to characterize the extent of this cold population we also identify the most poleward latitude of the cold ( $< 240$  eV) electron fluxes. These fluxes are typically highly structured and take on the appearance of flux islands in region of very low fluxes. This is in contrast to the more equatorial regions of the hot electron plasma sheet where flux dropouts in all electron channels are virtually absent.

The poleward boundary of the energetic protons is defined by the most poleward latitude at which  $> \sim 6$  keV proton fluxes were observed above instrument sensitivity level.

### **2.3 Particle acceleration structures**

Parallel electric fields at ionospheric altitudes are known to give rise to inverted V's, field aligned and trapped pitch angle distributions in the electron fluxes, and to upward flowing ions [Sharp et al]. These signatures in the particle distributions are therefore used for identifying and locating auroral acceleration structures. For the purpose of the present study the following ion and electron acceleration structures are identified from characteristic features in the ion and electron fluxes:

1. **Upflowing ion events (UFI)** with either field aligned (beams) or conical (conics) pitch angle distributions. Each contiguous region of ion upflow was characterized by its latitude and extent in latitude, typical energy range of the ions and the predominant pitch angle distribution. To be counted as a UFI event region, a pitch angle anisotropy with flux peaking in the upward direction was required to be present on at least two consecutive spins.

- 2.) **Electron pitch angle structures (EPAS)** with characteristic modulations as described in Sharp and Cladys and Sharp . Again each contiguous modulation region was characterized by its latitude of occurrence and its latitude extent. To be accepted as an event the modulations had to persist for at least two consecutive spin.

While UFI serve as indicators for the existence of electric field acceleration regions (primarily parallel) at altitudes below the satellite the latter provide identification of parallel electric fields above the satellite.

We refrain from directly using inverted V' signatures in the electron fluxes since the four point electron energy spectrum obtained by the LPARL experiment appears insufficient for unequivocally distinguishing acceleration signatures from purely spatial-temporal variation in the flux intensities. Instead we rely exclusively on the characteristic signatures in the electron pitch angle distributions for identifying parallel electric field acceleration above the satellite. A more detailed description of these signatures can be found in Sharp [19 ], and Cladys and Sharp [ ]. Since electron pitch angle modulation and inverted V signatures occur typically in the same regions this restriction is not expected to significantly affect the identification of acceleration regions above the satellite.

For both types of structures we record the low and high latitude edge of a contiguous region of the same type of characteristics. Here contiguous refers to observations on at least two consecutive spins. To be accepted as electron pitch angle modulation structures we require that the modulations occur for at least two consecutive spins in either of the four energy electron channels ( $> 70$  eV to 23.5 keV). Since UFI ions (beams)

are observed in the upward loss cone, and since the trapped population usually has a low flux, a single observation of UFI's is acceptable and assigned 1/2 spin width.

## 2.4 Analysis Method

The usual approach in statistical studies of auroral morphology has been to produce maps in absolute magnetic local time versus latitude coordinates. Here we propose to use a somewhat different approach in that we first identify the feats of interest, then renormalize to a reference coordinate system defined by the "plasma boundaries" and then carry out the statistical analyses in the relative coordinate system of the "reference feature".

Specifically, the transition feature adopted here is the region of hot trapped electron fluxes bounded at low latitudes by the EEB(hot) and at high latitudes by the PEB(hot) (see 3.2). The renormalization procedure is in essence a transformation to a coordinate system with origin at the EEB and unit length at the PEB. The latitude coordinates of all acceleration structures are mapped to this new "instantaneous" reference coordinate system defined by the absolute coordinates of the EEB and PEB on the same orbital pass. Following renormalization to this reference system the occurrence frequency distributions of auroral acceleration structures are derived in this relative coordinate system. For this purpose the hot electron region between the equatorward and poleward boundary was subdivided into 10 latitude bins for each auroral zone traversal. By summing over all orbits and normalizing, the occurrence frequency distributions as a function of normalized invariant latitude are obtained, from which first and second moments of the distributions and correlation analyses are derived.

Since auroral phenomena have significant local time dependencies, it is necessary to limit the data to be compared to a narrow range of magnetic local times. For the pre-midnight sector study the local time range of sampling was restricted to the range from 16 Hr to 20 HrMLT.

## 3. Results

Figure 2 provides an overview of the locations of the boundaries and of the latitude extent of the various regions as a function of time (abscissa). Arrows in the bottom panel indicate the time of the northern auroral zone traversal of the satellite. All orbits shown met the selection criteria outlined above. The shaded area in the center panel marks the region where the  $> \sim 1$  keV electron energy fluxes exceeded the instrument sensitivity threshold. At the poleward border (PEB) these fluxes always decrease to below instrument sensitivity level, while at the equatorward border (EEB) the fluxes often exhibit a minimum in energy flux. The location of the poleward proton (PIB) and the electron trapping boundaries (ETB) are indicated by the solid and dashed lines respectively. The solid vertical bars in denote the latitude extent of upward flowing ion (UFI) events and of electron pitch angle modulation structures (EPM). From the two uppermost panels (display of Kp and Dst) one can infer that two smaller magnetic storms occurred during the time period of this study. Overall the period was only moderately disturbed with average Kp  $\sim 3$ .

Evidence for particle acceleration was discernible in the large majority of orbits in this time period. Panels UFI and Ep in Fig. 2 indicate that particle acceleration occurred at least as frequently above the satellite as below. Furthermore, the large majority of acceleration structures occurred in conjunction with the presence of  $> \sim 1$  keV electron fluxes, or more precisely in the latitude region bounded by the EEB and the PEB. When UFI-structures were observed on occasion poleward of the PEB they were usually

accompanied by an enhanced flux of low energy electrons (flux islands). All EPM structures that occurred at latitudes poleward of the EEB are observed in the lowest electron energy channel, i.e. in the cold  $< 24$  keV electrons. These low energy electrons often extend further poleward than the hot electron fluxes, consistent with the observations reported by Sandahl and Lindqvist [1990]. As seen from Figure 1 ion and electron acceleration structures are much lesser frequent above the PEB.

The latitude distribution of acceleration structures relative to the EEB and PEB boundaries in the ambient hot electron plasma is given in Figure 3. From this result one can see that acceleration structures occur predominantly inside the hot electron plasma region (HEP). The occurrence frequency increases with relative latitude particularly in the first half of the HEP region. It maximizes near the poleward border reaching about 40 % for UFI events and 60% for EPM events. At the PEB the occurrence probability for both UFI and EPM acceleration structures drops abruptly and substantially. As seen from Figure 3 the electron trapping boundary (ETB) and poleward energetic proton boundary (PIB) are on the average located close to the PEB. These three boundaries are in fact well correlated (Figure ). While average location of the plasmopause is well equatorward ( $64.9^\circ$ ) of the EEB, the electric field reversal boundary ( $74.4^\circ$ ) determined by Mozer and Torbert [1980] from S3-3 data for a period covering the data of this study, is essentially collocated with the ETB of this study.

The statistical occurrence frequency distribution provides little information on the instantaneous latitude extent of particle acceleration structures. To illustrate this property we show in Figure 4 an occurrence frequency distribution of the "instantaneous" latitude extent of UFI and EPM structures in relation to the HEP region. The results indicate a surprisingly flat latitude width probability distribution up to a relative latitude width of  $\sim 70$  % of the HEP region. As a consequence acceleration structures extend on the average over about 40% of the HEP latitude width. Figure 5 indicates that the integrated probability for finding structures with width exceeding 40% is 50% of the orbits sampled.

From Figure 2 one can see that the location of the boundaries vary in latitude from one orbit to the next. However, the polar boundaries nevertheless track each other remarkably well. To examine whether a relationship exists between these boundaries we have conducted linear regression analyses of their latitude locations relative to one another. Particularly good correlations with significance  $< 1$  % (Fig 5a) are obtained between the high latitude boundaries investigated. Furthermore, the equatorward latitude boundaries of the particle acceleration structures and the HEP were also found to be well correlated (Fig 6b). These correlations suggest that the particle boundaries defined here represent coherent and consistent transition features, and that the same underlying cause and effect process are affecting them. In order to investigate the causes for these substantial variations in location we provide in Figures 6 c and d, scatter plots of the latitude locations of the equatorial hot electrons and the auroral acceleration boundary versus magnetic activity indices  $K_p$ . Here it is seen that the equatorward boundaries are well correlated with  $K_p$  (significance  $< 1$  %) while the high latitude boundaries do not exhibit significant correlation with  $K_p$ .

These dependencies on  $K_p$  are summarized in more accessible form in Figures 7 and 8. Figure 7 gives the latitude width of the HEP (a) and the integral width of particle acceleration structures normalized to the former. From Figure 5a it is evident that the HEP region increases from about  $4^\circ$  ILA width during magnetically quiet periods to about  $11^\circ$  ILA during active periods. At the same time the acceleration regions expand in latitude from about 20 % to about 70 % of the HEP latitude width.

## 4. Discussion

A distinct recurring feature of the dusk high latitude ionosphere at an altitude of about 1 Re is the hot electron plasma (HEP), which is characterized by trapped or precipitating fluxes of electrons with energies  $\geq 1$  keV. This population extends over a latitude width from about  $4^\circ$  ILA to about  $10^\circ$  ILA, increasing with Kp. At the low latitude side a boundary can relatively easily be identified from the decrease in energy flux of the energetic ( $\sim 1$  keV) electrons. This transition feature has the basic characteristics of the inner edge of the plasma sheet as observed in the equatorial plane. The latitude location of this transition feature in the  $> 1$  keV electrons is on average located about 1 L value further poleward than the locations reported by Horwitz [1986] for mixed LT ranging from 15 to 24 Hr. However, the present data were acquired primarily between 16 to 20 HR MLT, and hence a more poleward location is expected for the present data set. Furthermore, the plasma pause inferred from electric field data for a coincident data period is located further equatorward of the HEP boundary at about the expected latitude position. Thus, low latitude transition feature in the hot electron fluxes reported here is consistent with the low latitude extension of inner edge of the plasma sheet as observed in the equatorial plane. Hence, we conclude that low latitude boundary of the HEP as defined provides a reasonably good estimate for the location of the inner edge of the plasma sheet.

The poleward boundary of the HEP is not as distinctly defined as the low latitude edge since the energetic electron fluxes decrease more gradually and since the low energy electrons extend typically significantly further poleward. Nevertheless, the poleward boundary of the HEP edge follows closely the electric field reversal boundary determined by Mozer and Torbert [1981] from a larger S3-3 data base that included the orbits used in this study. In fact, this field reversal boundary is on average located only  $\sim 0.5^\circ$  further equatorward than the PEB (Mozer and Torbert, 1980). Two additional transition features are closely related to the PEB location; the PIB which is typically observed to extend further poleward by 0.13 HEP widths, and the ETB which is located at 0.81 of HEP width. The locations in latitude of these two "boundaries" are statistically well correlated with the PEB. Since these three features were independently derived from different signatures in the particle distributions, and since they appear to move in concert with each other as a result of magnetic activity suggests that all 3 features are distinct transition demarcations of polar ionospheric particle populations. The presence of energetic protons suggests that the plasma sheet extends at least up to the isotropic PIB.

In the equatorial plane, the plasma sheet is defined as the region of hot (keV) electron and proton fluxes, bounded by a substantial decrease in energy fluxes both at the low L and the L-sides. If the same basic definition were to be applied to the low altitude extension of plasma sheet, one would expect the PEB and the PIB to correspond closely to the high latitude, polar boundary of the plasma sheet. In this interpretation, the low energy electron fluxes, which tend to extend further poleward from the PEB as well as the PIB, give rise to a latitudinal thin region of the cold and highly structured electron population about  $1$  to  $2^\circ$  ILA wide. This extent exceeds the expected projected width of the plasma sheet boundary layer. Although a unique identification of the plasma sheet boundary layer is not possible from this data set, an interpretation for a location near the PIB - but within the region of highly structured cold electron fluxes would appear consistent with the equatorial observations of a region of colder less intense and highly structured fluxes.

As seen from Figure 3, ionospheric particle acceleration structures are strongly associated with the region of hot electron fluxes (HEP). Since the large majority of ionospheric particle acceleration structures occur (Figure 3) equatorward of the PEB, a

mapping to the plasma sheet appears indicated. Only a minority of acceleration structures are observed in the thin poleward region where the plasma sheet boundary layer is expected. Hence, in this view the large majority of ion and electron acceleration regions are located equatorward of the plasma sheet boundary layer in the plasma sheet proper.

Since particle acceleration is more frequent in the outer portion of the HEP plasma sheet (majority of events found in poleward 50% of HEP extent), this finding is not inconsistent with the interpretations of Wynnningham for a central (CPS) and boundary (BPS) plasma sheet. The central plasma sheet is distinct from the boundary plasma sheet in the sense that the former lacks the distinct features of intense inverted V electron precipitation structures. We note, however, that the distinction between BPS and CPS was intended to apply to the high latitude plasma sheet region and not may not necessarily apply to the more distant regions of the plasma sheet

From Fig 6 it is evident that auroral particle acceleration structures expand in latitude significantly during periods of high magnetic activity. This widening is primarily the result of an expansion to lower latitudes of the low latitude boundary of observable auroral particle acceleration features. Figure 1 indicates that low latitude boundary of the hot electrons moves toward lower L-values during the main phase and early recovery phase of the two magnetic storms. This substantial increase in width with magnetic activity implies an increase in injection of ionospheric ions into the plasma sheet.

## 5. Summary and Conclusions

1. Ion and electron acceleration structures extend over a substantial fraction of the hot electron "plasma sheet". The latitude extent of particle acceleration increases with geomagnetic activity, reaching on occasion at least ~75 % of the HEPwidth under disturbed conditions.
2. The occurrence frequency of particle acceleration increases gradually from the inner edge of the HEP "plasma sheet" to the poleward boundary where it decreases abruptly.
3. The latitudinal distribution of parallel electric field signatures above the satellite is similar to that of the upflowing ion structures, and agrees with the large scale parallel electric field in the plasma sheet reported by Mozer and Torbert [GRL, 1980].
4. The poleward boundary of precipitating energetic protons is on average located poleward of the 1 keV HEP, in agreement with the observations of Lyons et al. [JGR, 1988], who report that discrete aurora generally occur in regions of isotropic energetic ion precipitation.
5. Poleward of the 1 keV electron plasma sheet is one finds a latitudinal thin region of energetic proton precipitation (on average  $\sim 1^\circ$  equivalent to  $\sim 10\%$  of the HEPwidth) coincident with and a wider region of cold highly structured electron fluxes. A mapping of the "plasma sheet boundary layer" observed at  $> 20$  Re to this high altitude polar region seems appropriate..
6. At dusk and altitudes of  $\sim 1$  Re auroral ion and electron acceleration structures are located predominantly within the HEP "plasma sheet" region. Acceleration structures may occur anywhere from the low latitude edge to the high latitude boundary of the

HEP "plasma sheet" but with a clear preference for the high latitude 50% portion of the HEP.

7. On an orbit by orbit basis the latitude width of auroral particle acceleration exhibits large variations. However, this latitude extent increases both absolutely and relatively with respect to the HEP width with geomagnetic activity.
8. Based on the generally recognized association between discrete auroral arcs, parallel electric fields and ion and electron acceleration signatures in the particle distributions we conclude that a.) the high latitude HEP plasma sheet maps to the auroral oval, and b.) that the large majority of discrete auroral arc and inverted V acceleration structures occur within this HEP plasma sheet.

## FigureCaptions

Fig. 1: Orbit of S3-3 Satellite during sampling period used for this study showing principal magnetospheric plasma regions.

Fig. 2: Latitude extent of particle acceleration structures ( solid vertical bars) near dusk at high altitudes ( $> 6000$  km) during a two month acquisition period over the northern auroral zone. Shaded region represents the extent of hot ( $> \sim 1$  keV) electron fluxes ("Plasma Sheet"). The electron trapping boundary (ETB) and the poleward proton boundary (PIB) are indicated by the solid and dashed lines, respectively. Panel E shows the locations of electron pitch angle modulation structures, panel UFI the location of upward flowing ions (beams and conics).

Fig. 3: Occurrence frequency distribution of particle acceleration regions as a function of normalized invariant latitude. The "hot electron plasma sheet" was subdivided into 10 normalized latitude bins between the equatorward (EEB) and the polar boundary (PEB). The latitude locations of the acceleration regions were then mapped to this relative coordinate system. The upper panel gives the occurrence frequency for the inferred parallel electric fields regions above satellite (from EPAS), the lower one for the upflowing ion regions. The average relative location of the ETB is indicated by the arrow "e", while the PIB location is indicated by the arrow "p". The average location of the plasmopause was  $64.9^\circ$  and of the electric field reversal boundary  $74.4^\circ$  for a period that included the orbits used in the present study (Mozer and Torbert, GRL. 219, 1980).

Fig. 4: Statistical distribution of "instantaneous" latitude extent of acceleration structures in units of hot electron plasma sheet latitude width.

Fig. 5: Probability of latitude extent of acceleration structures exceeding a given fraction of the hot electron plasma sheet latitude width.

Fig. 6: Dependence of the latitude width of the hot electron plasma sheet (a) , and of particle acceleration structures (b) as a function of Kp index.

Fig. 7: Poleward and equatorward boundaries of hot plasma sheet electrons and locations of the most poleward and most equatorward edge of auroral particle acceleration regions as a function of Kp index.

Fig. 8: Schematic representation of the high latitude morphology of particle acceleration and plasma boundaries. Dawn side morphology is inferred from Viking observations [Quinn et al, Part 1]. Statistical frequency distribution of particle acceleration regions are schematically indicated by solid line and upward pointing arrow. Average ILA values for boundaries are indicated for reference.

## References

Baumjohann WJ, G. Paschmann, and C.A. Cattell, Average plasma properties in the

- central plasma sheet, *J. Geophys. Res.*, 94, 6597, 1989.
- Benett, E.L., M. Temerin, and F.S. Mozer, The distribution of auroral electrostatic shocks below 8000-km altitude, *J. Geophys. Res.*, 88, 7107, 1983.
- Birn, J., The geomagnetic tail, *Rev. of Geophys.*, p 1049, 1991.
- Coley, W.R., Spatial relationship of field-aligned currents, electron precipitation, and plasma convection in the auroral oval, *J. Geophys. Res.*, 88, 7131, 1983.
- Croley, D.R., P.F. Mizera, and J.F. Fennell, Signatures of a parallel electric field in ion and electron distributions in velocity space, *J. Geophys. Res.*, 83, 2701, 1978.
- Fairfield D.H., and A.F. Vinas, The inner edge of plasma sheet and the diffuse aurora, *J. Geophys. Res.*, 89, 841, 1984.
- Frank, L.A., Relationship of the plasma sheet, ring current, trapping boundary, and plasmopause near the magnetic equator and local midnight, *J. Geophys. Res.*, 76, 2265, 1971.
- Frank, L.A., and J.D. Craven, Imaging results from dynamics explorer I, *Rev. Geophys.*, 26, 249, 1988.
- Frank, L.A., Plasmas in the earth's magnetotail, *Space Sciences Reviews* 42, 211, 1985
- Galperin, Yu.I., and Ya.I. Feldstein, Auroral luminosity and its relationship to magnetospheric plasma domains, in *Auroral Physics*, ed. C.I. Meng, M.J. Rycoft, and L.A. Frank, Cambridge University Press, Cambridge, U.K., p. 207, 1991.
- Ghielmetti, A.G., R.G. Johnson, R.D. Sharp, and E.G. Shelley, The latitudinal, diurnal and altitudinal distributions of upward flowing energetic ions of ionospheric origin, *Geophys. Res. Lett.*, 5, 59, 1978.
- Ghielmetti, A.G., R.D. Sharp, E.G. Shelley, and R.G. Johnson, Downward flowing ions and evidence for injection of ionospheric ions into the plasma sheet, *J. Geophys. Res.* 84, 5781, 1979.
- Gorney, D.J., A. Clarke, D. Croley, J. Fennell, J. Luhmann, and P. Mizera, The distribution of ion beams and conics below 8000 km, *J. Geophys. Res.* 86, 83, 1981.
- Gussenhoven, M.S., D.A. Hardy, and N. Heinemann, Systematics of the equatorward diffuse auroral boundaries, *J. Geophys. Res.*, 88, 5692, 1983.
- Gussenhoven, M.S., D.A. Hardy, and N. Heinemann, The equatorward boundary of auroral ion precipitation, *J. Geophys. Res.*, 92, 3273, 1987.
- Hardy, D.A., M.S. Gussenhoven, and E. Hølemann, A statistical model of auroral electron precipitation, *J. Geophys. Res.*, 90, 4229, 1985.
- Hardy, D.A., M.S. Gussenhoven, and D. Brautigam, A statistical model of auroral ion precipitation, *J. Geophys. Res.*, 94, 370, 1989.
- Heelis, R.A., J.D. Winningham, W.B. Hanson, and J.L. Burch, The relationship between high-latitude convection reversals and the energetic particle morphology observed by atmospheric explorer, *J. Geophys. Res.*, 85, 3315, 1980.
- Hones, E.W. Jr., Plasma sheet behaviour during substorms in Magnetic Reconnection in Space and Laboratory Plasmas, *Geophys. Monograph* 30, Ed. By E.W. Jones Jr., *Am. Geophys. U.*, Washington DC, 178, 1984.
- Horwitz J.L., S. Menteer, J. Turnley, J.L. Burch, J.D. Winningham, C.R. Chappell, J.D. Craven, L.A. Frank, and D.W. Slater, Plasma boundaries in the Magnetosphere, *J. Geophys. Res.*, 91, 8861, 1986.
- Kamide, Y., and J.D. Winningham, A statistical study of the instantaneous nightside auroral oval: the equatorward boundary of electron precipitation as observed by the Isis 1 and 2 satellites, *J. Geophys. Res.* 82, 5573, 1977.
- Klumpar, D.M., A digest and comprehensive bibliography on transverse auroral ion acceleration, in *Ion Acceleration in the Magnetosphere*, Ed. T. Chang, *Geophys. Monograph* 38, 389, 1987.
- Lennartsson W., R.D. Sharp, E.G. Shelley, and R.G. Johnson, Ion composition and energy distributions during 10 magnetic storm, *J. Geophys. Res.*, 86, 4628, 1981.
- Lennartsson W. and R.D. Sharp, Substorm effects on the plasma sheet ion compo-

- sition on March 22, 1979 (CDAW 6), *J. Geophys. Res.* 90, 1243, 1985.
- Lin, C.S., and R.A. Hoffmann, Observations of inverted-V electron precipitation, *Space Sci. Rev.* 33, 415, 1982.
- Lyons, L.R., and D.S. Evans, An association between the discrete aurora and energetic particle boundaries, *J. Geophys. Res.*, 89, 2395, 1984.
- Maikita, K., C.-I. Meng, and S.-I. Akasofu, The shift of the auroral electron precipitation boundaries in the dawn-dusk sector in association with geomagnetic activity and interplanetary magnetic field., *J. Geophys. Res.*, 88, 7967, 1983.
- Maikita, K., C.-I. Meng, and S.-I. Akasofu, Temporal and spatial variations of the polar cap dimensions inferred from the precipitation boundaries, *J. Geophys. Res.* 90, 2744, 1985.
- Maikita, K., C.-I. Meng, and S.-I. Akasofu, Latitudinal electron precipitation patterns during large and small IMF magnitudes for Northward IMF conditions, *J. Geophys. Res.* 93, 97, 1988.
- Mauk, B.H., and C.-I. Meng, Characterisation of geostationary particle signatures based on the injection boundary model, *J. Geophys. Res.* 88, 3055, 1983.
- Mauk, B.H., and C.-I. Meng, The aurora and middle magnetospheric processes in Auroral Physics, ed. C.-I. Meng, M.J. Rycoft, and L.A. Frank, 223, Cambridge University Press, Cambridge, U.K. 1991.
- McIlwain, C.E. Substorm injection boundaries, in Magnetospheric Physics, ed. B.M. McCormac, D. Reidel, Hingham, MA., p. 143, 1974.
- McPheron, R.L., C.T. Russell, and M.P. Aubrey, Satellite studies of magnetospheric substorms on August 15, 1968, Phenomenological model for substorms, *J. Geophys. Res.*, 78, 3131, 1973.
- Meng, C.-I., and K. Maikita, Dynamic variation of the polar cap, in Solar Wind-Magnetospheric Coupling, ed. By Y. Kamide and J. Slavin, Terra Scientific Pub. Co., Tokyo, 605, 1986.
- Meng C.-I., and B.H. Mauk, Global auroral morphology: Quadrennial report to the I.U.G.G. on U.S. contributions, *Rev. Geophys.*, 1028, April 1991.
- Mizera, P.F., J.F. Fennell, D.R. Croley Jr., A.L. Vampola, F.S. Mozer, R.B. Torbert, M. Temerin, R.L. Lysak, M.K. Hudson, C.A. Cattell, R.G. Johnson, R.D. Sharp, A.G. Ghielmetti, and P.M. Kintner, The aurora inferred from S3-3 particles and fields, *J. Geophys. Res.* 86, 2329, 1981.
- Mozer, F.S., and R.B. Torbert, An average parallel electric field deduced from the latitude and altitude variations of the perpendicular electric field below 8000 km, *Geophys. Res. Lett.* 7, 219, 1980.
- Newell, P.T., C.I. Meng, and D.A. Hardy, Low altitude observations of dispersionless substorm plasma injection, *J. Geophys. Res.*, 92, 10063, 1987.
- Newell, P.T., and C.-I. Meng, Overview of electron and ion precipitation in the Auroral Oval, in Auroral Physics, ed. C.I. Meng, M.J. Rycoft, and L.A. Frank, Cambridge University Press, Cambridge, U.K., p. 203, 1991.
- Newell, P.T., and C.I. Meng, Mapping the dayside ionosphere to the magnetosphere according to particle precipitation characteristics, *Geophys. Res. Lett.* 19, 609, 1992.
- Nishida, A., S.J. Bame, D.N. Baker, G. Gloekler, M. Scholer, E.J. Smith, T. Teravasa, and B. Tsurutana, Assessment of the boundary layer model of the magnetospheric substorm, *J. Geophys. Res.*, 93, 5579, 1988.

- sition on March 22, 1979 (CDAW 6), *J. Geophys. Res.* 90, 1243, 1985.
- Lin, C.S., and R.A. Hoffmann, Observations of inverted-V electron precipitation, *Space Sci. Rev.* 33, 415, 1982.
- Lyons, L.R., and D.S. Evans, An association between the discrete aurora and energetic particle boundaries, *J. Geophys. Res.*, 89, 2395, 1984.
- Maikita, K., C.-I. Meng, and S.-I. Akasofu, The shift of the auroral electron precipitation boundaries in the dawn-dusk sector in association with geomagnetic activity and interplanetary magnetic field., *J. Geophys. Res.*, 88, 7967, 1983.
- Maikita, K., C.-I. Meng, and S.-I. Akasofu, Temporal and spatial variations of the polar cap dimensions inferred from the precipitation boundaries, *J. Geophys. Res.* 90, 2744, 1985.
- Maikita, K., C.-I. Meng, and S.-I. Akasofu, Latitudinal electron precipitation patterns during large and small IMF magnitudes for Northward IMF conditions, *J. Geophys. Res.* 93, 97, 1988.
- Mauk, B.H., and C.-I. Meng, Characterisation of geostationary particle signatures based on the injection boundary model, *J. Geophys. Res.* 88, 3055, 1983.
- Mauk, B.H., and C.-I. Meng, The aurora and middle magnetospheric processes in *Auroral Physics*, ed. C.-I. Meng, M.J. Rycoft, and L.A. Frank, 223, Cambridge University Press, Cambridge, U.K. 1991.
- McIlwain, C.E. Substorm injection boundaries, in *Magnetospheric Physics*, ed. B.M. McCormac, D. Reidel, Hingham, MA., p. 143, 1974.
- McPheron, R.L., C.T. Russell, and M.P. Aubrey, Satellite studies of magnetospheric substorms on August 15, 1968, Phenomenological model for substorms, *J. Geophys. Res.*, 78, 3131, 1973.
- Meng, C.-I., and K. Maikita, Dynamic variation of the polar cap, in *Solar Wind-Magnetospheric Coupling*, ed. By Y. Kamide and J. Slavin, Terra Scientific Pub. Co., Tokyo, 605, 1986.
- Meng C.-I., and B.H. Mauk, Global auroral morphology: Quadrennial report to the I.U.G.G. on U.S. contributions, *Rev. Geophys.*, 1028, April 1991.
- Mizera, P.F., J.F. Fennell, D.R. Croley Jr., A.L. Vampola, F.S. Mozer, R.B. Torbert, M. Temerin, R.L. Lysak, M.K. Hudson, C.A. Cattell, R.G. Johnson, R.D. Sharp, A.G. Ghielmetti, and P.M. Kintner, The aurora inferred from S3-3 particles and fields, *J. Geophys. Res.* 86, 2329, 1981.
- Mozer, F.S., and R.B. Torbert, An average parallel electric field deduced from the latitude and altitude variations of the perpendicular electric field below 8000 km, *Geophys. Res. Lett.* 7, 219, 1980.
- Newell, P.T., C.I. Meng, and D.A. Hardy, Low altitude observations of dispersionless substorm plasma injection, *J. Geophys. Res.*, 92, 10063, 1987.
- Newell, P.T., and C.-I. Meng, Overview of electron and ion precipitation in the Auroral Oval, in *Auroral Physics*, ed. C.I. Meng, M.J. Rycoft, and L.A. Frank, Cambridge University Press, Cambridge, U.K., p. 203, 1991.
- Newell, P.T., and C.I. Meng, Mapping the dayside ionosphere to the magnetosphere according to particle precipitation characteristics, *Geophys. Res. Lett.* 19, 609, 1992.
- Nishida, A., S.J. Bame, D.N. Baker, G. Gloekler, M. Scholer, E.J. Smith, T. Teravasa, and B. Tsurutana, Assessment of the boundary layer model of the magnetospheric substorm, *J. Geophys. Res.*, 93, 5579, 1988.

- Rostocker, G., and T. Eastman, A boundary layer model for magnetospheric substorms, *J. Geophys. Res.*, **92**, 12187, 1987.
- Rostocker, G. Overview of observations and models of auroral substorms, in *Aurora* 1 Physics, ed. C.I. Meng, M.J. Rycoft, and L.A. Frank, 257, Cambridge University U.K. 1991.
- Sandahl, I., and P-A. Lindqvist, Electron populations above the nightside auroral oval during magnetic quiet times, *Planet. Space Sci.*, **38**, 1031, 1990.
- Sisco, G.L., What determines the site of the auroral oval in *Auroral Physics*, ed. C.I. Meng, M.J. Rycoft, and L.A. Frank, Cambridge University Press, Cambridge, U.K. p. 141, 1991.
- Sharp, R.D., R.G. Johnson, and E.G. Shelley, Energetic particle measurements from within ionospheric structures responsible for auroral acceleration processes, *J. Geophys. Res.*, **84**, 480. 1979.
- Sharp, R.D., A.G. Ghielmetti, R.G. Johnson, and E.G. Shelley, Hot plasma composition results from the S3-3 spacecraft, in *Energetic Ion Composition in the Earth's Magnetosphere*, Ed. R.G. Johnson, Terra Scientific Publishing Co., Tokyo, and D. Reidel, Dordrecht, Holland, 167, 1983.
- Torbert, R.B., C.A. Cattell, F.S. Mozer, and C.-I. Meng, The boundary of the polar cap and its relation to electric fields, field-aligned currents, and auroral particle precipitation, in *Physics of Auroral Arc Formation*, ed. A.I. Akasofu and J.R. Kan, *Geophys. Monograph 25*, AGU, Washington, D.C., p. 143, 1981.
- Weimer, D.R. Substorm Time Constants, submitted to *Geophys. Res. Lett.* 1992
- Winningham, J.D., F. Yasuhara, S.-I. Akasofu, and W.J. Heikkila, The latitudinal morphology of 10 e V to 10 ke V electron fluxes during magnetically quiet and disturbed times in the 2100-0300 MLT sector, *J. Geophys. Res.*, **80**, 3148, 1975.
- Yau, A.W., B.A. Whalen, W.K. Peterson, and E.G. Shelley, Distribution of upflowing ionospheric ions in the high-altitude polar cap and auroral ionosphere, *J. Geophys. Res.*, **89**, 5507, 1984.

ORBIT OF S3-3 SATELLITE FROM AUG 18 TO SEP 29, 1976

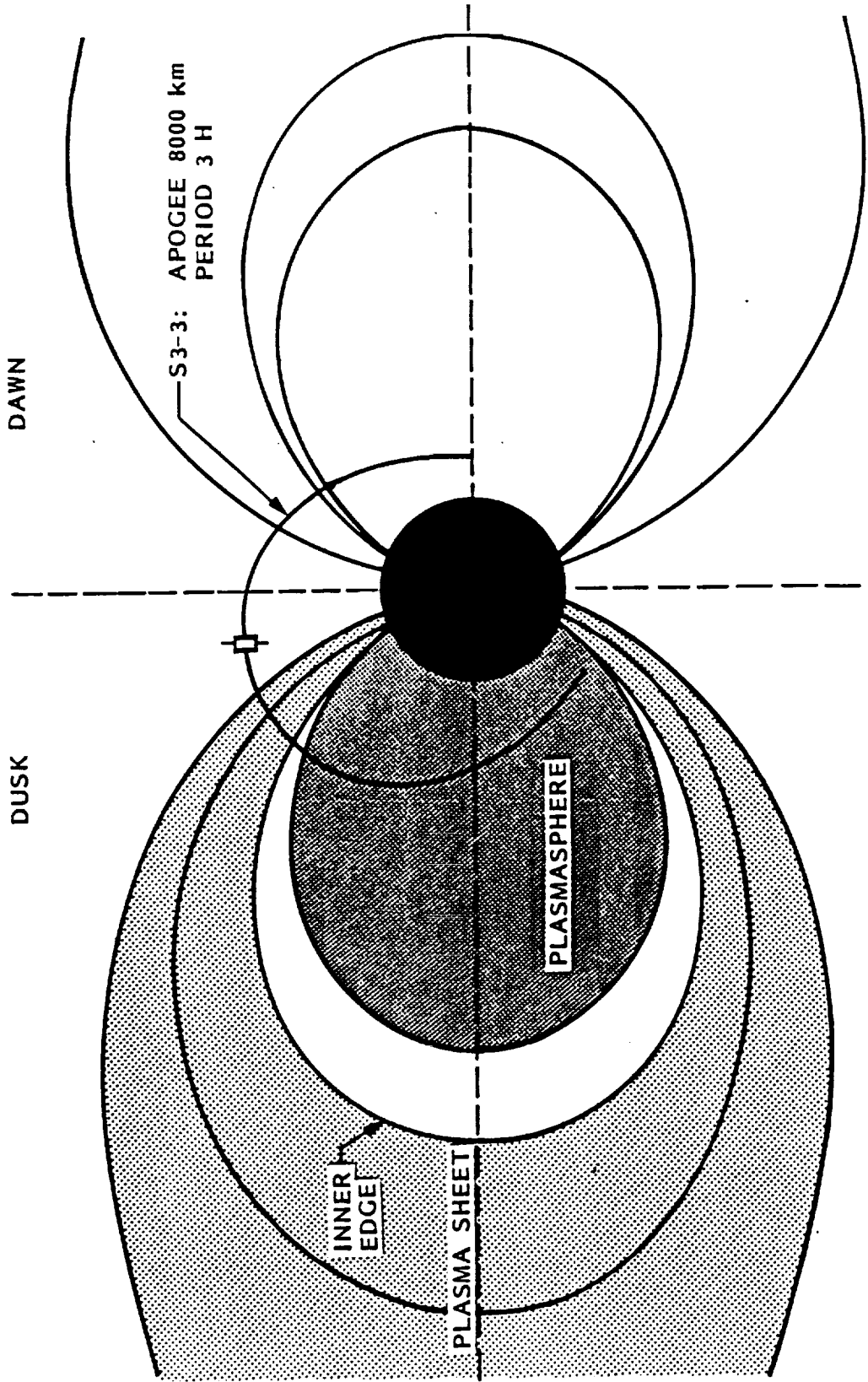
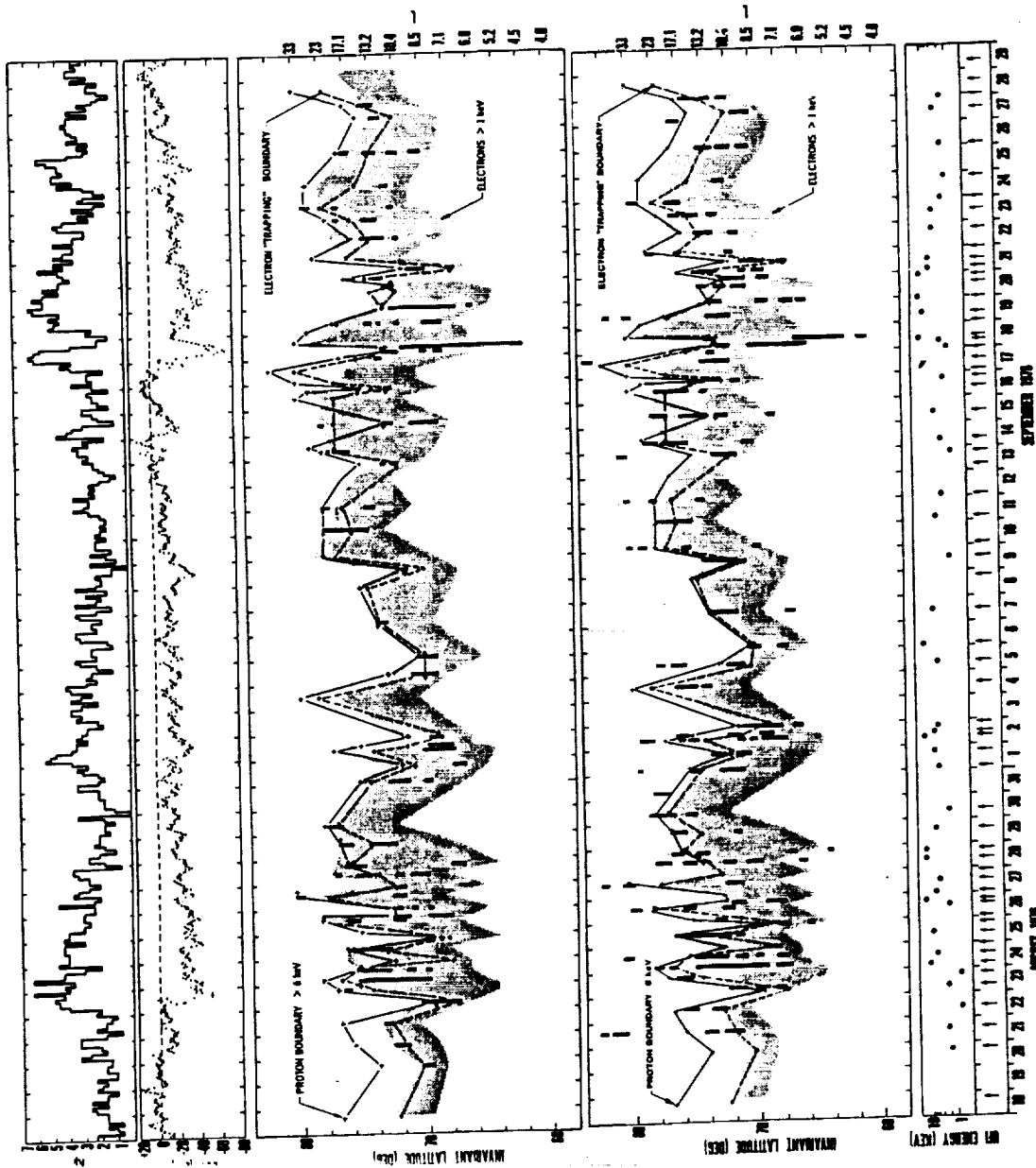


Fig 1



**Figure 2:** Latitudinal locations of particle acceleration regions (denoted by black vertical bars) as observed during 63 high altitude (>6000 km) traversals of the northern auroral zone. Shaded region indicates extent of  $> 1$  keV electron fluxes ("Plasma Sheet"). "Electron trapping boundary" is the most poleward latitude at which upward and downward loss cones were visible in the pitch angle distributions. "Proton boundary" is the most poleward latitude at which energetic ( $> 6$  keV) protons were observed.

Panel UFI: Upward flowing ions (beams and conics).

Panel  $E_{||}$ : Parallel electric fields above the satellite inferred from the electron pitch angle distributions (see Cladis and Sharp JGR, p.6564, 1979).

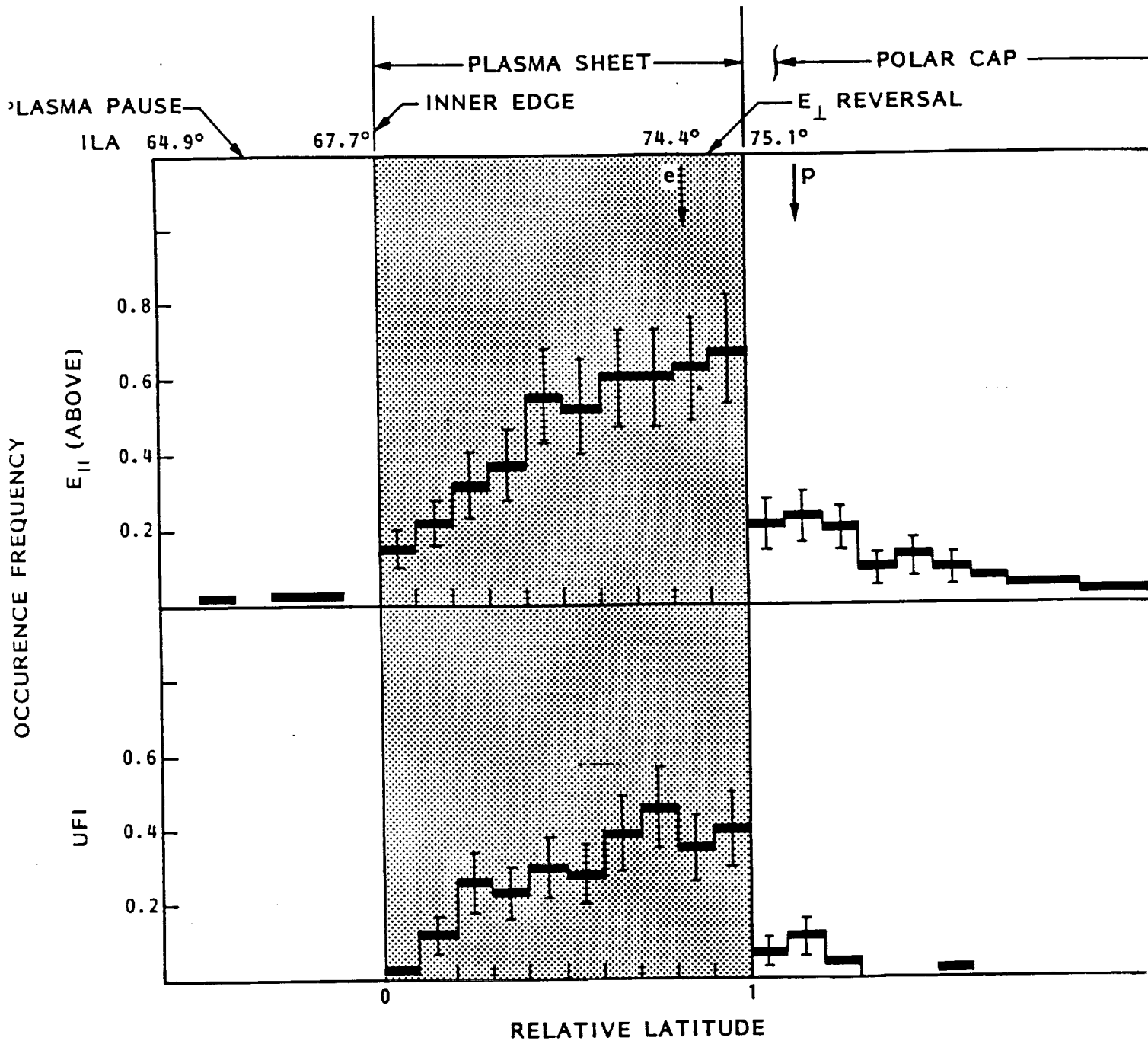


Fig. 2:

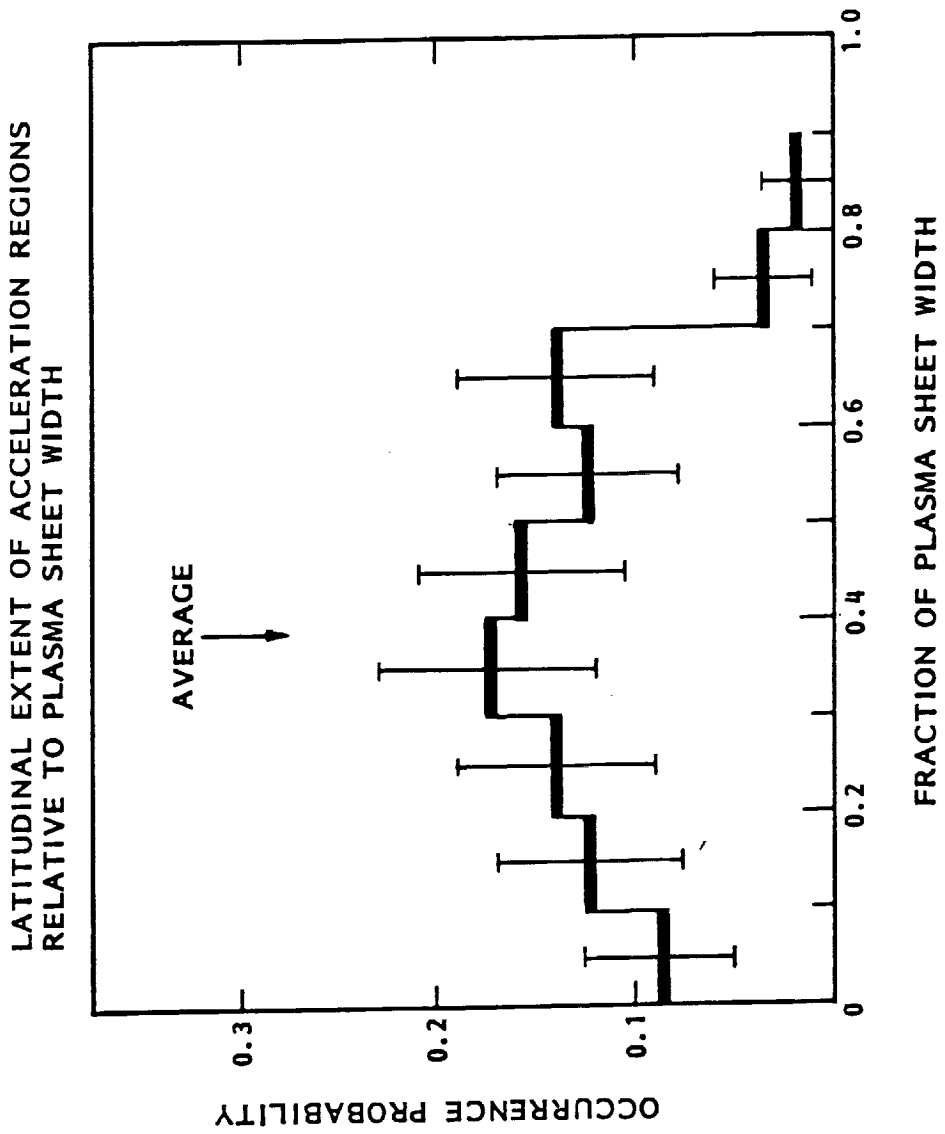
Occurrence frequency of particle acceleration regions as a function of normalized invariant latitude. The "Plasma Sheet" between the equatorward inner edge and the polar boundary of  $>1$  keV electron fluxes was subdivided into 10 normalized latitude bins for each auroral zone traversal. The latitude locations of the acceleration regions were then mapped to this relative coordinate system.

Upper panel: Parallel electric fields above satellite inferred from electron pitch angle distributions  
 Lower panel: Upflowing ions (beams and conics)

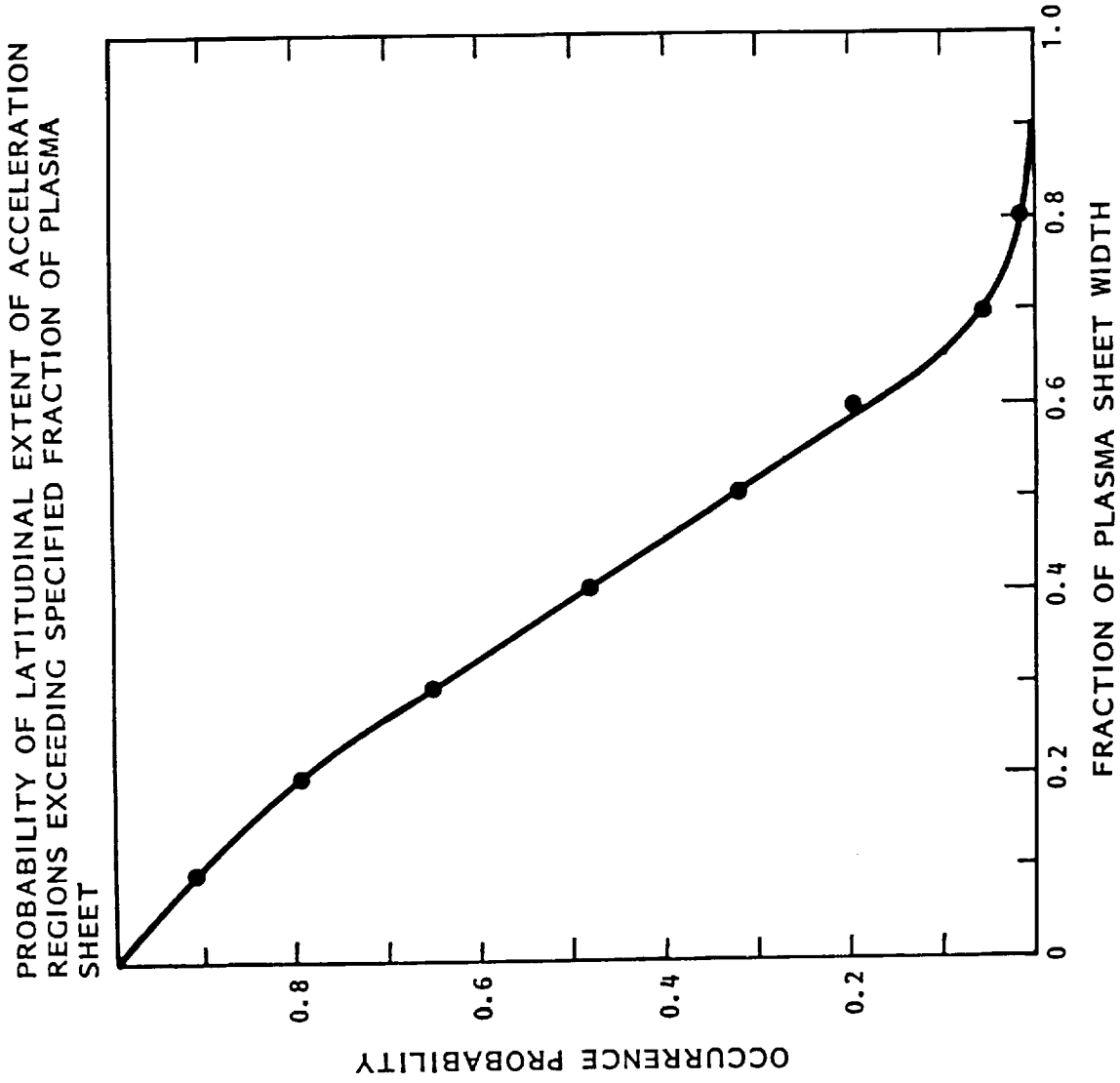
$e_{||}$  => poleward location of anti loss cones in electron pitch angle distributions

$p$  => " boundary of  $> 6$  keV isotropic precipitating protons.

Plasmapause (64.9 deg) and electric field reversal boundary (74.4 deg) are from Mozer and Torr (Geophys. Res. Lett., p219, 1980), for a data period covering period.



4  
 Figure 3: Distribution of "instantaneous" width of acceleration regions in units of plasma sheet latitudinal width.



5

**FIGURE 6:** Same data as Figure 5, integrated to show the probability of the ion acceleration regions exceeding given latitudinal fractions of the plasma sheet.

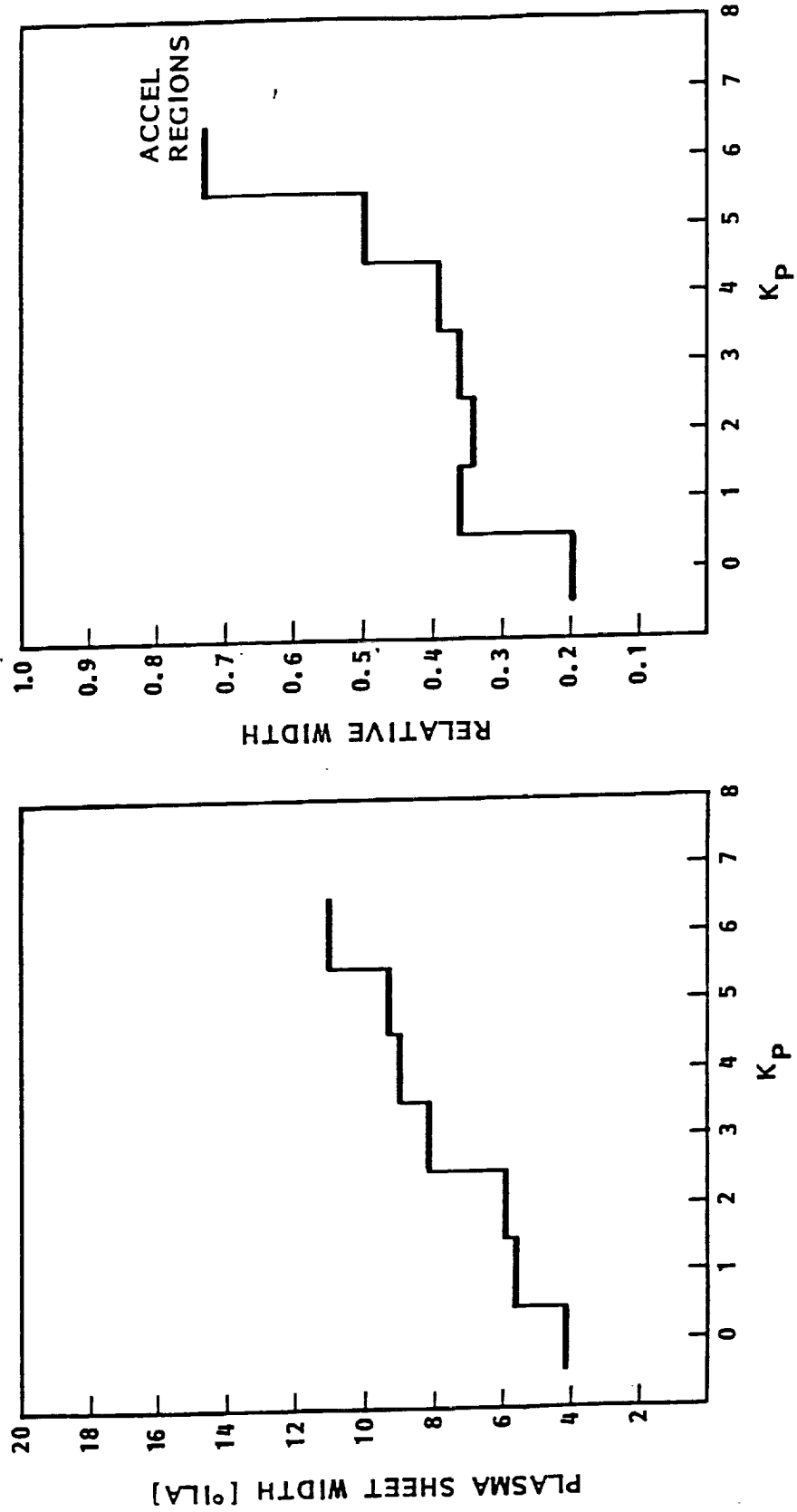


Figure 6: Width of plasma sheet (a), and relative width of particle acceleration regions (b) as a function of Kp index.

Spatial Relationships  
of Auroral Particle Acceleration Relative to High Latitude Plasma  
Boundaries

Part II : "Post-Midnight Local Time Sector"

J.M. Quinn and A.G. Ghielmetti

**Contents**

1. Introduction.....	3
2. Data Selection and Analysis.....	4
3. Results .....	6
4. Discussion.....	8

## ABSTRACT

Ion data from the Viking satellite are used to identify auroral acceleration structures in the post-midnight local time sector. The locations of these ion acceleration regions are compared to four particle boundaries inferred from the transition features in the isotropic electron and ion fluxes. In the post-midnight region, acceleration structures are often observed to occur over a substantial width in latitude ( $5^\circ$ ) and are statistically centered about a boundary representing the poleward edge of contiguous

energetic ion fluxes. The position of this boundary with respect to other article boundaries and as a function of magnetic activity are also examined.

## 1. Introduction

In this paper we consider the latitudinal location of auroral region ion acceleration relative to various signatures of the surrounding plasma populations. Previous statistical studies have determined the absolute latitudinal positions of energetic ion outflow as a function of local time. Similar statistical investigations have been performed for most other key auroral zone phenomena such as electron precipitation, electric field structure, currents, and auroral emissions. However, only a limited number of detailed case studies have explored the "instantaneous" *relative* location of upflowing ionospheric ions in the context of other auroral features. Thus, although we know statistically the independent latitudinal positions of many auroral zone plasma features, there is not a sound basis upon which to draw conclusions regarding their "typical" latitudinal relationship to auroral ion acceleration. In this paper we hope to provide a bridge between the statistical and the detailed case studies by examining the "instantaneous" relative locations of ion outflow to other plasma signatures over a fairly large number (89) of polar orbital cuts by the Viking satellite.

The identification of auroral zone ion acceleration has generally relied upon two techniques: the direct measurement of upflowing ions, observed above or within the acceleration region, and the inference of upward directed

parallel electric fields above the spacecraft from electron pitch angle signatures (e.g. Cladis and Sharp, 1979; Sharp et al. 1979). The statistical morphology of the directly measured outflowing ions has been extensively characterized using data from S3-3 (Ghielmetti et al., 1978; Gorney et al., 1981; Sharp et al., 1983) and DE (Yau et al., 1984; Yau et al., 1985; Collin et al., 1988). The average local time and invariant latitude distributions presented in these studies are generally consistent with the auroral oval, although there is significant variation with the upflowing ions' energy and pitch angle character (beam vs. Conic). While these studies show that the absolute latitudinal range within which ion acceleration is observed is quite large (degrees), examples from individual orbits show the instantaneous latitudinal extent to be highly variable, from less than 1 degree to greater than 5 degrees (e.g. Ghielmetti et al., 1978).

Case studies addressing the latitudinal location of auroral ion acceleration with respect to the high latitude signatures of various plasma populations have provided a good deal of insight into the magnetospheric context of the ion acceleration process (Winningham et al., 1975; Heelis et al., 1980; Mizera et al., 1981). However, the identification of latitudinal structures observed by polar orbiting satellites with features that have been identified in the equatorial region is made difficult by uncertainties in the magnetic field mapping and by differences in the measurements imposed by orbital constraints. An excellent review by Feldstein and Galperin summarizes the plethora of (Sometimes conflicting) terminology that has been applied to plasma sheet morphology and highlights the difficulties in identifying a self consistent picture.

In this paper we present the results of a statistical study of the latitudinal location of ion upflow with respect to the signatures of the ambient plasma population, as observed by the Viking in apogee passes through the dawn-side auroral zone. A companion paper will present complementary dusk-side results from S3-3 (Ghielmetti et al., 1990).

## **2. Data Selection and Analysis**

The data used in this study were acquired by the V3 hot plasma instrument complement aboard the polar orbiting Viking spacecraft. This satellite was launched into a highly eccentric orbit with a perigee of 817 km, apogee of 13500 km, and inclination of 98 degrees in early 1986. The spacecraft was spinning in a near cartwheel mode at 3 rpm and hence full pitch angle distributions were obtained every 20 seconds. The instrument included a set of three electron spectrometers orientated at 70, 90 and 110 degrees that covered the energy range from 10 eV to 40 keV in less than 0.6 sec. Two ion spectrometers mounted at 90 degrees relative to the spin axis measured the total ion fluxes in the range from 40 eV to 40 KeV with the same temporal resolution. More complete descriptions of the instrumentation are given in Sandahl et al (1985).

The data selected for this investigation were acquired between April 24 and June 2 1986. During this 40 day period, the satellite orbit crossed the dawn side auroral oval at high altitudes ( $> 11000$  km), thus maximizing the probability for ion accelerations below the satellite (Ghielmetti et al., 1978, Gorney et al., 1981). For the present study, we required the absence of cusp like dispersion signatures in the ion fluxes. A total of 89 orbits that met the above criteria provided near uniform sampling of the local time region from 06.00 to 08.00 MLT, and latitudes from 65 to 80 degrees ILA (Figure 1). The period selected is characterized by generally low magnetic activity and is near the minimum of the solar cycle.

Ion and electron microfiche data in the form of color coded energy-time spectrograms were visually scanned for signatures of upward flowing ions (UFI), and for presence of isotropic fluxes above a threshold level. For the purpose of the

present study an UFI region required the existence of a pitch angle anisotropy with flux peaking in the upward direction on at least two consecutive spins for ion energies  $> 100$  eV. Each contiguous region of ion upflow was characterized by its extent in latitude, the typical energy range of the UFI's and the predominant pitch angle type (field aligned or conical).

In addition to identifying UFI regions within each orbit, we also defined several latitudinal boundaries for the ambient plasma. In the more equatorward high latitude region ( $< 70$  deg ILA) the keV electron fluxes observed with Viking typically decreased gradually with decreasing latitude and did not exhibit a well defined flux discontinuity. Similarly, the fluxes of  $> 1$  keV ions were typically seen down to the lowest latitudes inspected ( $< 65$  deg) without any evidence of systematic discontinuities. As a result it is not meaningful to define an "inner boundary" based on some arbitrary flux level in the particle distributions. However, at higher latitudes both the electron and ion fluxes at energies  $> 1$  keV typically exhibit one or several flux discontinuities that can be used to define a "poleward boundary". Although structured fluxes of lower energy ( $1$  keV) electrons were often seen to extend even further poleward, only the energetic plasma boundaries were used for the present study.

To characterize latitudinally the location of the isotropic energetic plasma we therefore introduce the following "boundary" definitions

1. **Continuous Electron Boundary (CEB)**: The most poleward latitude at which  $\geq 1$  keV electron fluxes were observed continuously at lower latitudes (no gaps or flux dropouts at lower latitudes)
2. **Poleward Electron Boundary (PEB)**: The most poleward latitude at which  $\geq 1$  keV electron fluxes were observed. (By definition, PEB is  $\geq$  CEB).
3. **Continuous Ion Boundary (CIB)**: Same as CEB, but for ions.

#### 4. Poleward Ion Boundary (PIB): Same as PIB, but for ions.

In identifying the above boundaries a flux discontinuity was defined as a decrease in the energy flux below the sensitivity threshold of the instrument lasting for multiple ( $\geq 2$ ) satellite spins. Figure 2 schematically illustrates the boundary definitions together with typical features observed in the electron and ion fluxes.

To illustrate the ion end electron structures encountered, we present in Figure 3 a sample energy-time spectrogram for a near dawn auroral zone pass. In this particular case the CEB was identified at 75.5 degrees ILA and the PEB at 80.3 degrees, while the ion boundaries were located at 76.4 degrees (CIB) and 80.0 degrees (PIB). Upward flowing ions with field aligned pitch angle distributions are seen to occur on every spin between about 17.22 and 17.32 hr UT. This contiguous region of ion upflow shows consistently field aligned distributions (beams) with energies from  $\sim 0.1$  to 2 keV, while the flux intensities and energy distributions vary noticeably. In the present survey, the distinction between beams and conics, and the energy of UFI, are not utilized, although as described above they were included in the database.

### 3. Results

Figure 4 provides an overview of the latitudinal locations of upflowing ions observed over the period of study, together with the simultaneously identified location for two of the particle boundaries. For each orbit, the invariant latitude range(s) over which upflowing accelerated ions were observed are indicated by vertical bars. In many of the orbits multiple, latitudinally distinct, regions of UFI were seen. As many as five separate regions of UFI were resolved during individual orbits, indicative of the significant amount of structure in the acceleration process. Out of the 89 orbits studied, only 4 contained no regions of UFI.

The polar boundary of continuous energetic ions (CIB), as defined in Section 2, is represented on Figure 4 as a solid line, drawn to connect the individual sampling points. The corresponding boundary for electrons (CEB) is indicated by shading at latitudes below the boundary. The ion boundary is seen to be generally poleward of the electron boundary, with the average displacement between the two of 1.5 degrees.

Several features of Figure 4 are immediately apparent. First, for individual passes, the identified regions of UFI extend over a latitudinal range of many degrees. Second, the UFI seem to follow the locations of the isotropic particle boundaries as they move in latitude. Finally, the two, independently

determined, particle boundaries track each other fairly closely. A quantitative analysis supports each of these points, as will be shown below.

The occurrence frequency distribution in one degree invariant latitude bins is presented in Figure 5 for the UFI identified in this study. Both the latitudinal distribution and probability values are in general agreement with previous statistical studies of the latitudinal distribution of UFI (eg. Gorney et al., 1981; Yau et al., 1984; Collin et al., 1988). Although differences in instrument energy coverage, altitude range of sampling, and phase of solar cycle make a quantitative comparison somewhat difficult, we can conclude that the distribution of UFI identified in this study are consistent with the previous results.

As with previous studies of UFI, the Viking data confirm that the acceleration processes that are responsible for ion outflow are active a large fraction of the time. Even a raw distribution in invariant latitude shows probabilities greater than 60 % in three of the 1 degree latitude bins.

Much more sharply peaked distributions are obtained when the UFI position is examined relative to the particle boundaries identified for each orbit. Figure 6 shows the UFI occurrence frequency in 1 degree latitudinal bins relative to the CIB. It is clear from comparison with Figure 5 that a significant degree of ordering is obtained by relating the UFI positions to the CIB. Clearly, it is not surprising that such an ordering should be obtained with respect to this boundary, or with respect to any other feature that would be expected to move with the overall enlargement and contraction of the auroral oval. Indeed latitudinal peaks that are nearly as sharp, but with offsets, are obtained when the UFI positions are measured with respect to the CEB.

The magnitudes of the 1 degree UFI probabilities represented in Figure 6 are quite impressive. The peak probability of 88% that is uncovered by comparison to the continuous ion boundary position is significantly higher than has been determined by previous studies of ion upflow, which have looked only at absolute latitude distributions and thus were subject to significant smearing by common latitudinal motion of auroral structures. It is worth noting, however, that even with the good ordering shown in Figure 6, there are still 5 1-degree bins with higher than 50% probability for observing UFI.

From inspection of Figure 4, one might suspect that the approximately 5° FWHM distribution with respect to the continuous ion boundary (Figure 6) results primarily from the intrinsic latitudinal width of the instantaneous UFI distribution. In order to verify this, we show in Figure 7 the occurrence frequency for the integrated latitudinal width of UFI from each orbit. This width represents only the sum of the individual UFI segments from each orbit (not the difference between minimum and maximum latitudes at which UFI were observed). As anticipated, Figure 7 shows that the integrated regions of UFI most commonly occupy an "instantaneous" latitudinal extent of 4 to 5 degrees.

The isotropic particle boundaries defined in Section 2 were derived from independent observations. In order to examine whether a relationship exists between these boundaries we provide in Figure 8a a scatter plot of the latitude of the continuous ion- and the continuous electron boundaries (CIB and CEB) for all orbits within the data set. A linear regression analysis yields a correlation coefficient  $r = 0.86$ , with  $n=85$ , which is significant at  $<0.01\%$ . This good correlation suggests that the two boundaries move in concert. The CEB is, on average, offset in the equatorward direction from the CIB by  $1.5^\circ$ . The correlations between the other isotropic boundaries are not as good but are nevertheless significant.

Further analysis shows that the isotropic particle boundaries move equatorward with increasing magnetic activity. Both the CIB and CEB are well correlated with  $K_p$  and AE. A particularly good correlation is observed for the CIB (Figure 8b) with  $r=0.64$  at  $<0.01\%$  significance. A weaker but significant correlation with magnetic activity is observed for the integrated latitudinal width of the UFI regions from each orbit (Figure 9).

#### 4. Discussion

The above observations suggest that the continuous isotropic particle boundaries as defined in Section 2 may be useful as a relative markers of the latitudinal location of the auroral zone "plasma sheet" plasma. They do not provide a definitive position of the polar cap boundary nor can they be used to infer the instantaneous width of the plasma sheet. However, in the absence of a clear identification of plasma sheet "edges", which is particularly difficult in the dawn local time sector, these boundaries provide useful flags for locating the position of UFI's and may prove equally useful in defining the relative locations of other auroral zone phenomena. The technique provided a successful ordering of UFI using plasma features in terms of magnetospheric morphology. It is hoped that this method can be used equally well for comparing the relative positions of other auroral zone features.

We note several features about the UFI distributions. First, the observed occurrence distributions presented in Figures 5-7 must be regarded as lower limits to the frequency of auroral acceleration. The UFI technique and the selection criteria used here identify only those acceleration regions that generate  $UFI > 100$  e V at altitudes below the spacecraft. Observations at higher altitudes (e.g. Collin et al., 1988) demonstrate that a significant amount of acceleration can occur above the Viking apogee.

One of the key results is that the "instantaneous" integrated width of UFI is typically 4 to 5 degrees in latitude (Figure 7). This is not surprising from examination of individual particle spectrograms that have been published

over many years from various polar orbiting spacecraft. However the mapping of this extended acceleration region into the outer magnetosphere remains a challenge. In particular, models which assume that UFI are primarily generated within very narrow structures, such as are associated with discrete arcs, are difficult to reconcile with the data presented here.

A further result of interest in considering the magnetospheric context of the acceleration regions is the shape of the UFI latitudinal distribution with respect to the CIB (Figure 6). In particular, the distribution is quite symmetric about this boundary, as opposed, for instance, to rising to a cutoff at the boundary. This contrasts to the results of a similar study performed in the dusk local time sector using data from S3-3 (Ghielmetti et al., 1990). If one assumes that the CIB is or is related to, a geophysically meaningful plasma boundary, then one might consider that the acceleration is related to processes occurring at or near to the boundary. It is hoped that future comparisons of these results with similar studies for other auroral zone phenomena will help to shed light on both the mapping into the outer magnetosphere and on the causality between the UFI regions and the plasma structures.

## References

Cladis, J.B. and R.D. Sharp, Scale of electric field along magnetic field in an inverted V event, *J. Geophys. Res.*, 84, 6564, 1979.

Collin, H.L., W.K. Peterson, J.F. Drake, and A.W. Yau, The helium components of energetic terrestrial ion upflows: their occurrence, morphology and intensity, *J. Geophys. Res.*, 93, 7558, 1988.

Feldstein, Y.I., and Y.I. Galperin, The auroral luminosity structure in the high-latitude upper atmosphere: Its dynamics and relationship to the largescale structure of the earth's magnetosphere, *Rev Geophys.*, 23, 217, 1985.

Ghielmetti, A.G., R.G. Johnson, R.D. Sharp, and E.G. Shelley, The latitudinal, diurnal, and altitudinal distributions of upward flowing energetic ions of ionospheric origin, *Geophys. Res. Lett.*, 5, 59, 1978.

Ghielmetti, A.G., J.M. Quinn, and R.N. Lundin, Extent and relative locations of auroral acceleration regions II: Pre-Midnight Sector, to be submitted to *J. Geophys. Res.*, 1990.

Gorney, D.J., A. Clarke, D. Croley, J. Fennell, J. Luhmann, and P. Mizera, The distribution of ion beams and conics below 8000 km, *J. Geophys. Res.*, 86, 83, 1981.

Heelis, R.A., J.D. Winningham, W.B. Hanson, and J.L. Burch, The relationship between high-latitude convection reversals and the energetic particle morphology observed by atmospheric explorer, *J. Geophys. Res.*, 85, 3315, 1980.

Mizera, P.F., J.F. Fennell, D.R. Croley Jr., A.L. Vampola, F.S. Mozer, R.B. Torbert, M. Temerin, R.L. Lysak, M.K. Hudson, C.A. Cattell, R.G. Johnson, R.D. Sharp, A.G. Ghielmetti, and P.M. Kintner .... The aurora inferred from S3-3 particles and fields, *J. Geophys. Res.*, 86, 1219, 1981.

Sandahl, I., L. Eliasson, and R. Lundin, The hot plasma spectrometers on Viking, KGI Rep. 077, Kiruna Geophysical Institute, Feb. 1985.

Sharp, R.D., A.G. Ghielmetti, R.G. Johnson, and E.G. Shelley, Hot plasma composition results from the S3-3 spacecraft, in *Energetic Ion Composition in the Earth's Magnetosphere*, Ed. R.G. Johnson, Terra Scientific Publishing Co., Tokyo, and D. Reidel, Dordrecht, Holland, 167, 1983.

Winningham, J.D., F. Yasuhara, S.-I. Akasofu, and W.J. Heikkila, The latitudinal morphology of 10 eV to 10 KeV electron fluxes during magnetically quiet and disturbed times in the 2100-0300 MLT sector, *J. Geophys. Res.*, 80, 3148, 1975.

Yau, A.W., B.A. Whalen, W.K. Peterson, and E.G. Shelley, Distribution of upflowing ionospheric ions in the high-altitude polar cap and auroral ionosphere, *J. Geophys. Res.*, 89, 5507, 1984.

Yau, A.W., E.G. Shelley, W.K. Peterson, and L. Lenchyshyn, Energetic auroral and polar ion outflow at DE 1 altitudes: magnitude, composition, magnetic activity dependence, and long-term variations, *J. Geophys. Res.*, 90, 8417, 1985.

### **Figure Captions**

FIGURE 1. Invariant latitude and magnetic local time orbit tracks of Viking for the 89 auroral zone crossings analyzed in this study.

FIGURE 2. Schematic spectrogram illustrating the energetic plasma boundary definitions used in this study. CEB and CIB are poleward boundaries of latitudinally contiguous fluxes at energies greater than 1 keV for electrons and ions respectively. PEB and PIB are poleward most limits of all fluxes with energies greater than 1 keV.

FIGURE 3. Spectrogram of electron (top panel) and ion (bottom) panel fluxes during one of the orbits of the study period.

FIGURE 4. Latitudinal locations of observed upflowing ions from each orbit are indicated by vertical bars. Many orbits contain multiple, distinct regions in which UFI were observed. The poleward boundary of contiguous isotropic energetic ions is indicated by the solid line. The poleward boundary of contiguous energetic electrons is denoted by shading below the boundary.

FIGURE 5. Occurrence frequency of upflowing ions in 1 degree bins of invariant latitude. Background shading in 5 degree increments, is provided to guide the eye.

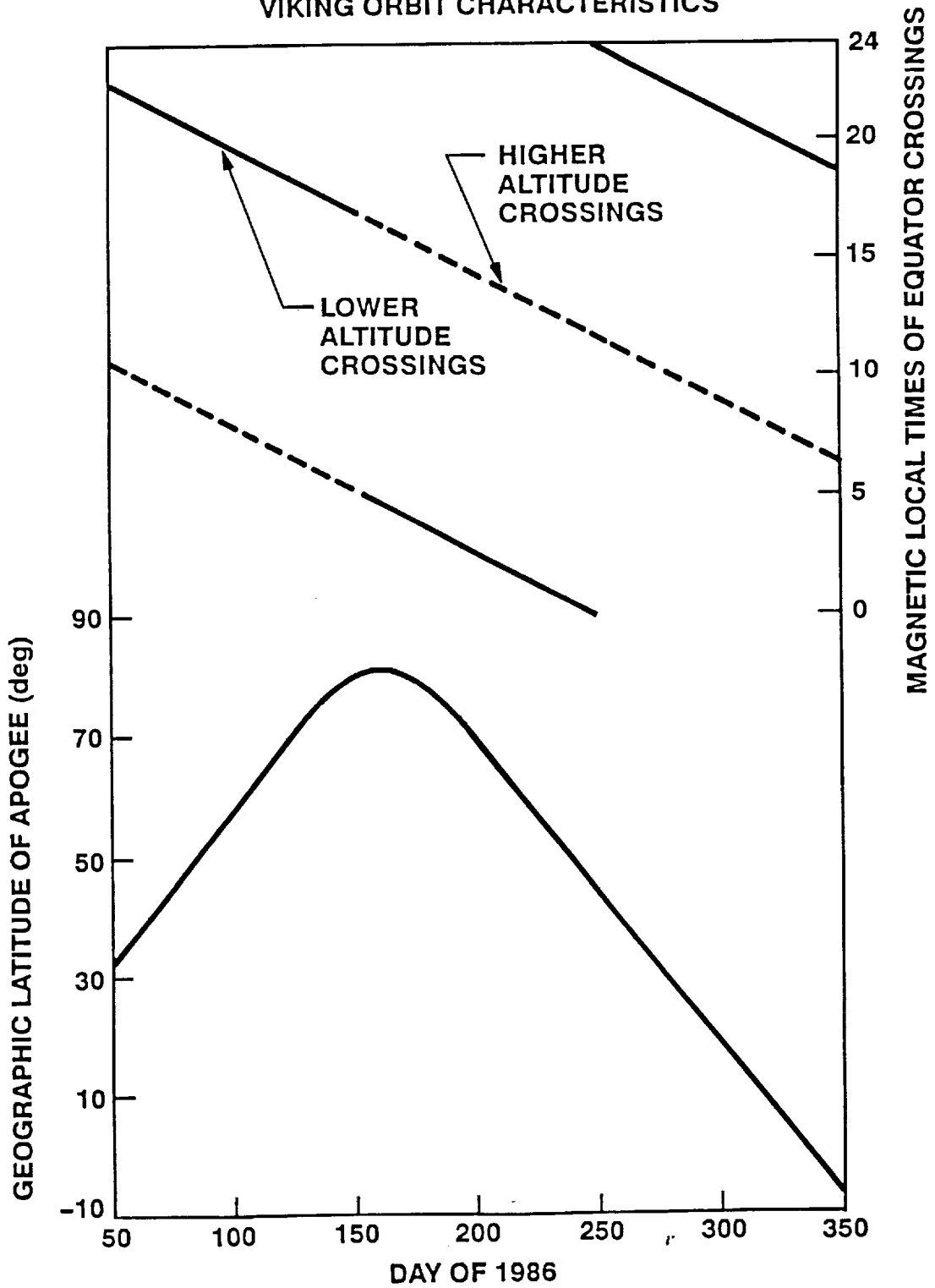
FIGURE 6. Occurrence frequency of upflowing ion in 1 degree bins relative to "instantaneous" position of poleward boundary of continuous energetic (1 keV) ions. The distribution with respect to this boundary is significantly more peaked than the raw distribution in invariant latitude (Figure 3).

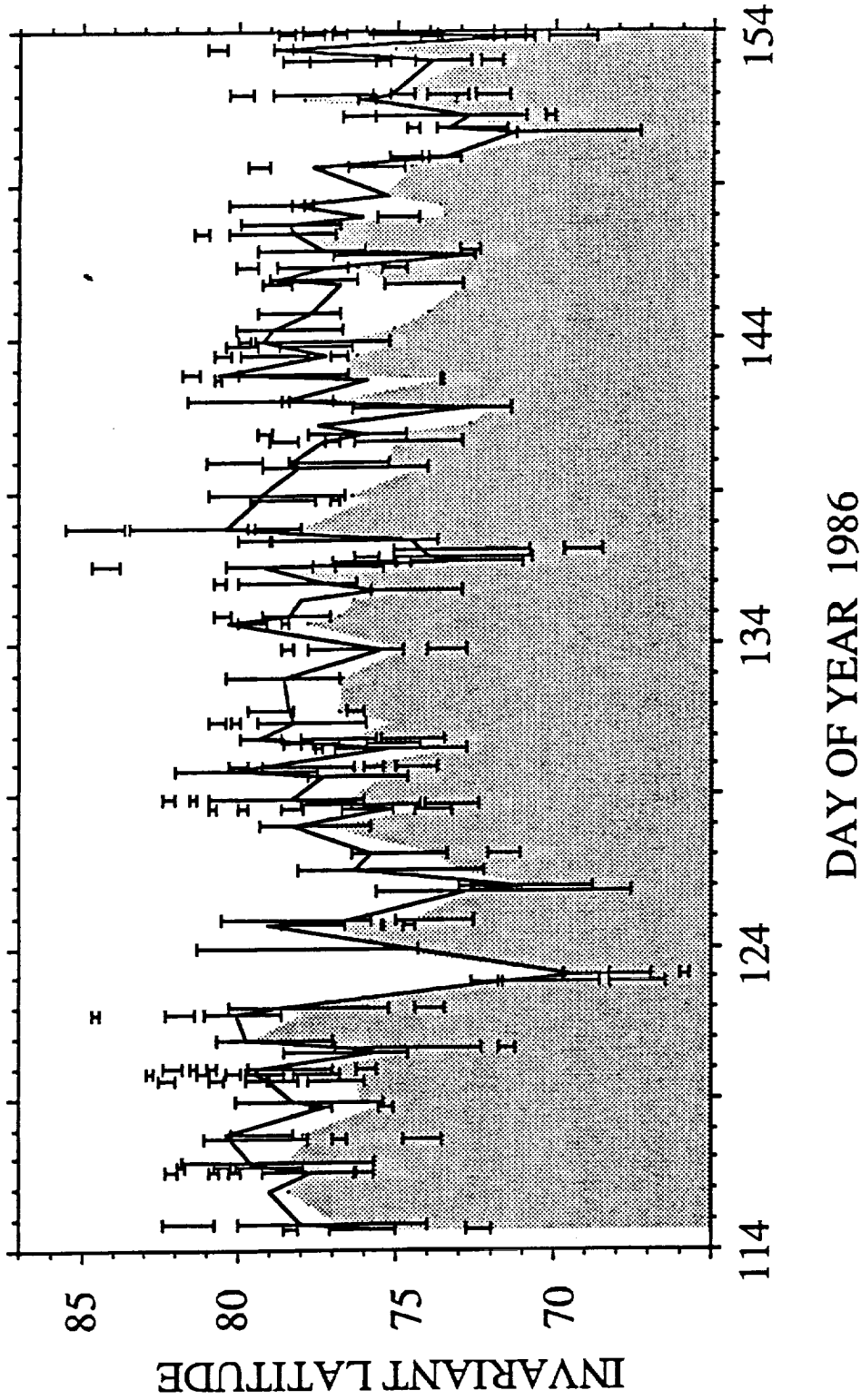
FIGURE 7. Occurrence frequency of the integrated latitudinal width of all regions of upflowing ions for each pass.

FIGURE 8. Scatter plots with linear regression fits for the Continuous Ion Boundary vs the Continuous Electron Boundary (top panel); and for the Continuous Ion Boundary vs the AE magnetic activity index (bottom panel).

FIGURE 9. Scatter plot of integrated width of upflowing ion regions vs magnetic activity index AE.

# VIKING ORBIT CHARACTERISTICS





**Figure 2:** Latitudinal locations of upward ion acceleration regions (denoted by black vertical bars) as observed during 89 high altitude (>11000 km) traversals of the northern auroral zone. Shaded region indicates region of contiguous > 1 keV electron fluxes. Solid line indicates poleward boundary of contiguous energetic (> 1 keV) ion fluxes (CIB).

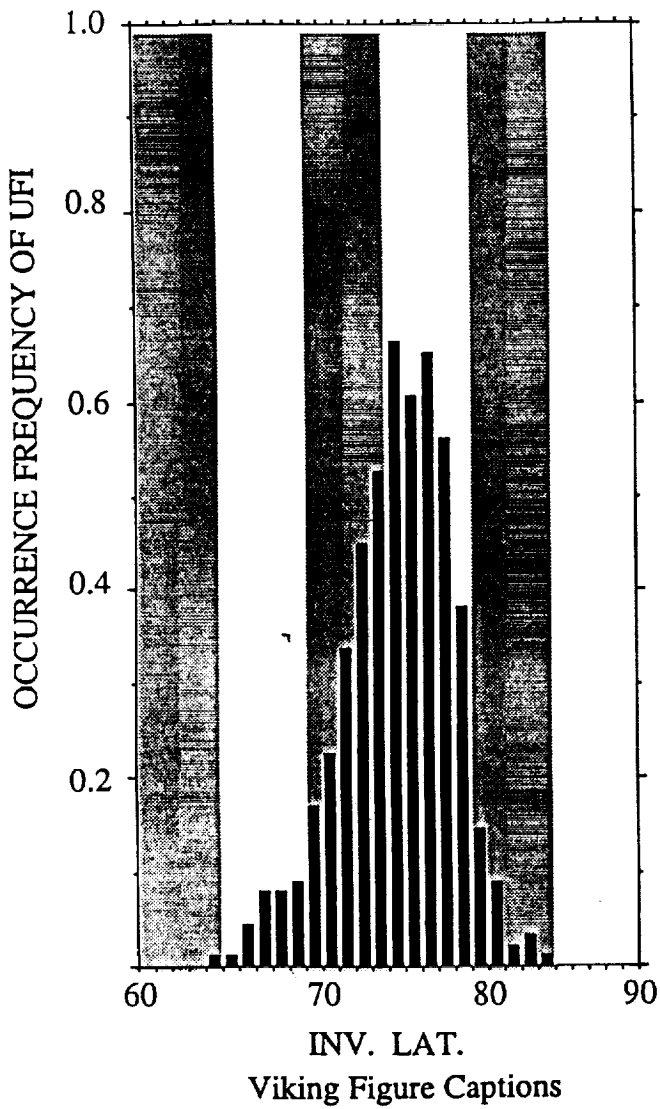


Figure 3:  
Occurrence frequency of UFI (beams and conics) in 1° bins of invariant latitude.

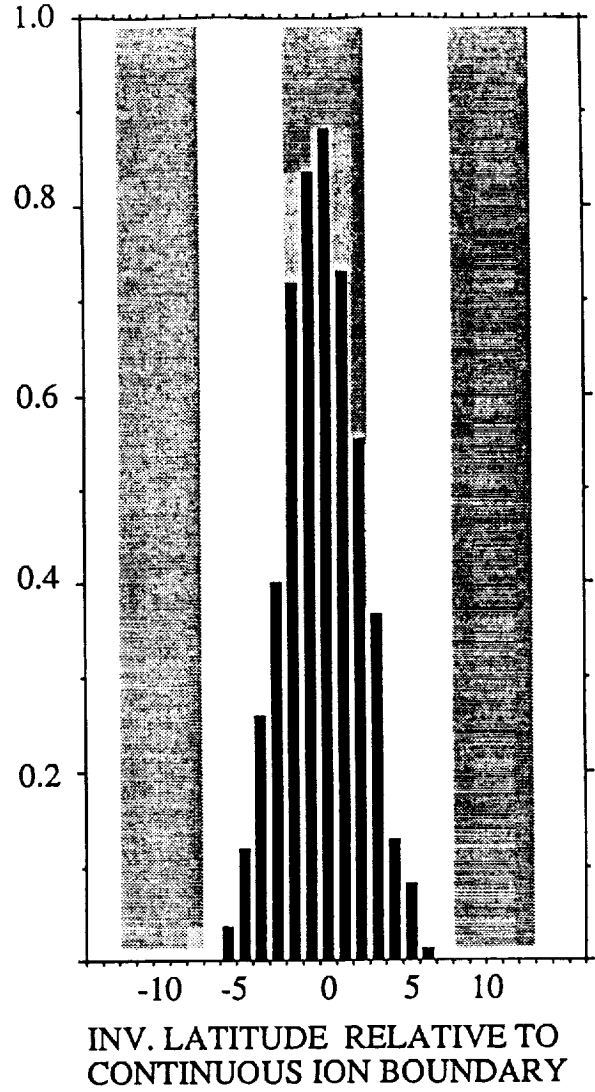
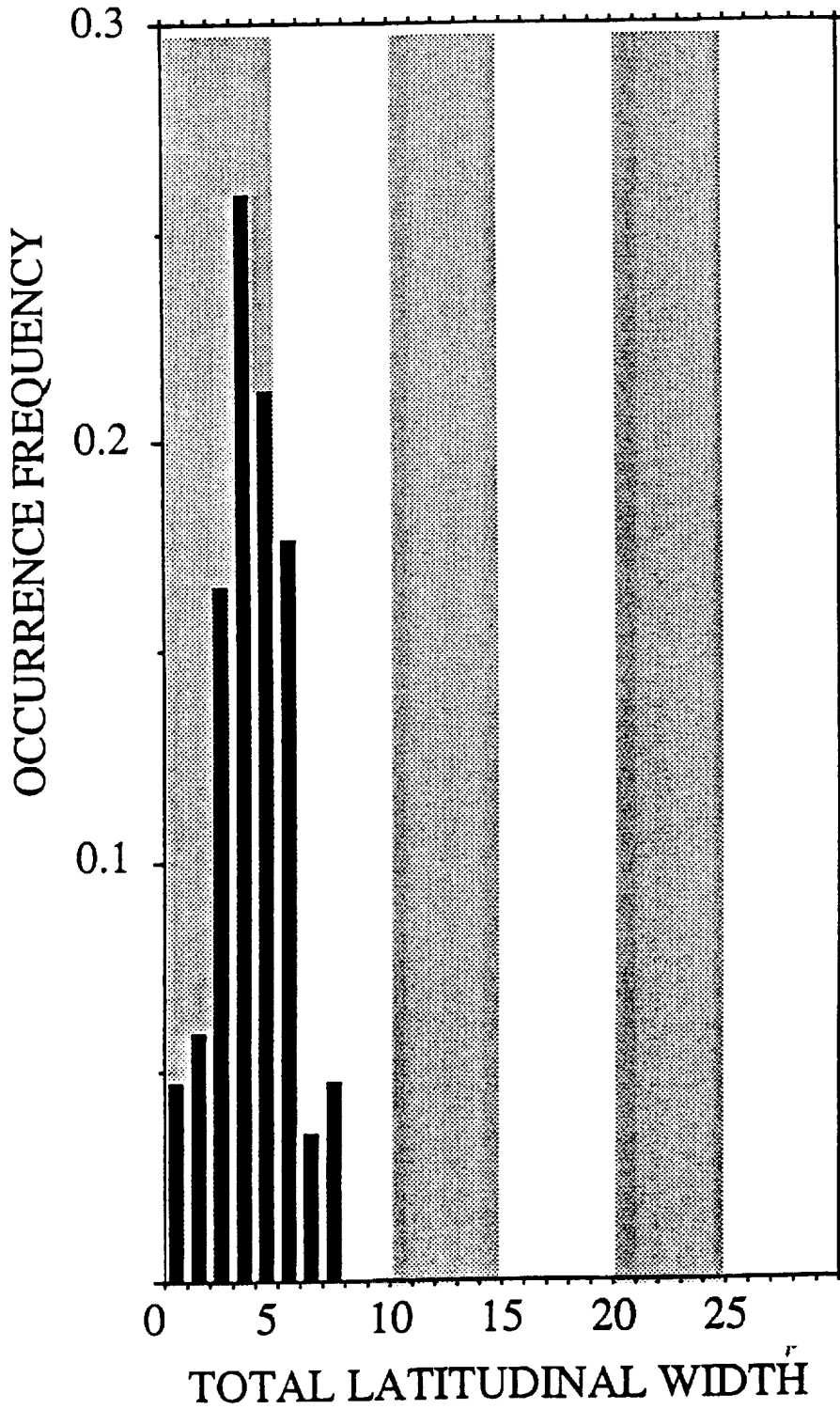
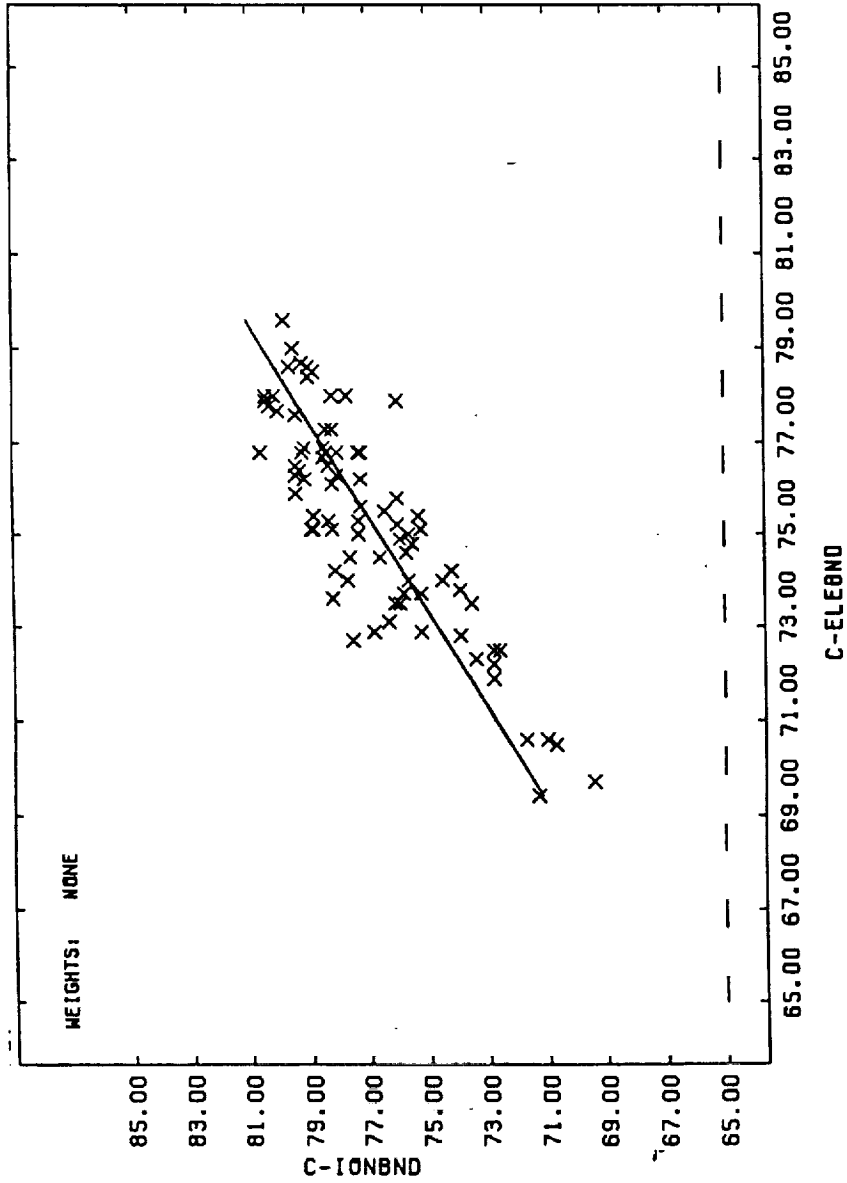


Figure 4:  
Occurrence frequency of UFI (beams and conics) in 1° bins of invariant latitude relative to the "instantaneous" latitude location of the contiguous ion boundary (CIB).



**Figure 5:**  
 Occurrence frequency of integrated instantaneous latitudinal width of ion upflow (beams and conics) during each auroral zone traversal. Average width is 4.1° ILA. Maximum latitude extent over which UFI's existed (most poleward - most equatorward border) is about 1° larger.



**Figure 6:** Scatter plot of invariant latitude of "contiguous ion boundary" (CIB) versus "contiguous electron boundary" (CEB) with regression line.

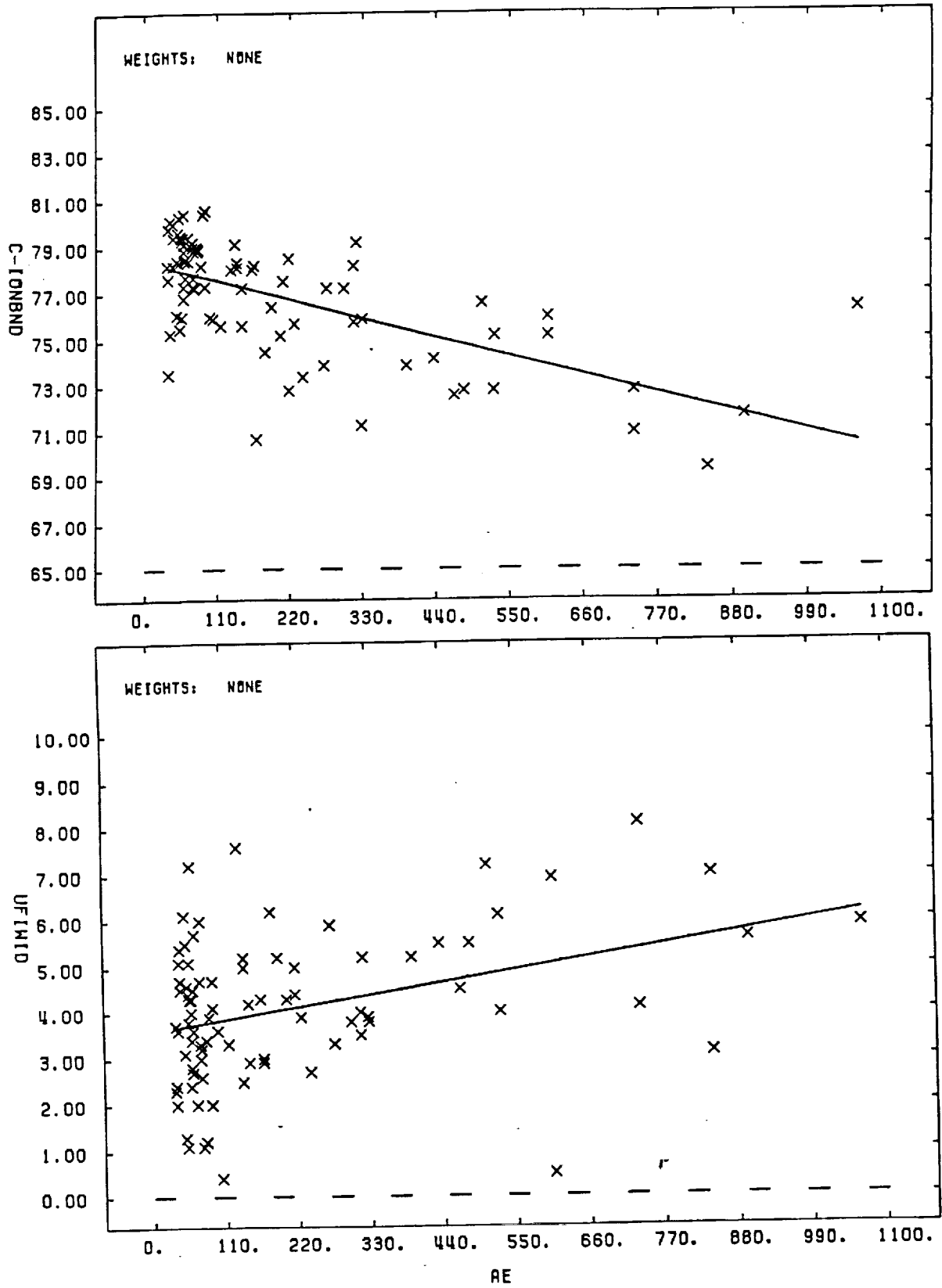


**Figure 7:** Latitude location of "contiguous ion boundary" (CIB) (a), and width of ion unflow regions (b) as a function of AE magnetic